THE RELATIONSHIP BETWEEN LITTORAL DRIFT RATE

AND

THE LONGSHORE COMPONENT OF WAVE ENERGY FLUX

APPROVED BY SUPERVISORY COMMITTEE:

THE RELATIONSHIP BETWEEN LITTORAL DRIFT RATE AND THE LONGSHORE COMPONENT OF WAVE ENERGY FLUX

by

RICHARD LEE WATSON, A.B., M.A.

DISSERTATION

Presented to the Faculty of the Graduate School of

The University of Texas at Austin

in Partial Fulfillment

of the Requirements

for the Degree of

DOCTOR OF PHILOSOPHY

THE UNIVERSITY OF TEXAS AT AUSTIN

May, 1975

A C K N O W L E D G E M E N T S

I would like to express my appreciation to Dr. Alan J. Scott, Dr. E. Gus Fruh, and Dr. R.L. Folk for their help in serving on the dissertation committee. Special thanks go to Dr. E. William Behrens who supervised the research and chaired the examining committee. The work could not have been accomplished without the help of Steven Frishman, Jerry Kier, and other graduate students who aided me in the collection of field data. Richard Moore of the Marine Science Institute kindly provided a program for statistical analysis of the data. Judith Watson drafted the dye concentration maps.

Financial support for my stay at the University of Texas was provided in the form of teaching assistantships in the Department of Geological Sciences, an Environmental Sciences Interdisciplinary Grant from Environmental Health Engineering, the Texaco Fellowship in Geology, summer support from Union Oil Company provided through the Geology Foundation of the University of Texas at Austin and other support from the Geology Foundation.

Research expenses were supported by a subvention funds grant from the Graduate School, and a Geological Society of America Grant in Aid of Research.

THE RELATIONSHIP BETWEEN LITTORAL DRIFT RATE

AND

THE LONGSHORE COMPONENT OF WAVE ENERGY FLUX

Publication No. _____

Richard Lee Watson, Ph.D.
The University of Texas at Austin, 1975

Supervising Professor: E. William Behrens

Quantitative prediction of littoral drift, the longshore transport of sediment in the surf zone of beaches is highly useful in the design of coastal engineering works such as harbor entrances, groin fields, and beach nourishment programs. Two approaches have been developed to arrive at predictor equations relating the rate of littoral drift to the longshore component of incident wave energy flux. The first method requires determination of net littoral drift by survey of beach erosion or accretion in the vicinity of a jetty or other structure which is a total barrier to littoral drift and relates the rate of transport so derived to long term wave records.

A second approach which relies on newly developed fluorescent tracer techniques has been developed

recently by several workers. Fluorescent dyed sand is released in the surf and is sampled in a grid pattern after a short period of transport. The volume rate of littoral drift is the product of the dye centroid velocity, the width of the surf zone, and the thickness of the mobile layer of sediment. Application of density and pore space corrections provides the immersed weight rate of transport. The incident wave energy flux is determined with a recording wave gage placed outside of the surf zone, and the longshore component of the wave energy flux is determined from measurement of the angle of incidence of the waves with the beach at the wave breakpoint. This method was used for the present study.

There are at present only four sets of quantitative field data on littoral drift including the data gathered in this study. Two sets have been measured by each of the above methods. Multiple regression analysis of the variables, wave energy flux, immersed weight transport rate, and mean grain diameter for the data gathered in the present study as well as the previously published data indicate that there is little or no effect of mean grain diameter on the rate of littoral drift within the sand size range.

The immersed weight transport (I) is related to

the longshore component of wave energy flux (P_a) by the following relationship for the Texas beaches studied.

$$\text{Log}_{10}(I) = 0.51\ \text{Log}_{10}(P_a) + 2.53\ .$$

A more general relationship based on all existing field data (Watts, 1953; Caldwell, 1956; Komar, 1970; and this study) is as follows:

$$\text{Log}_{10}(I) = 0.875\ \text{Log}_{10}(P_a) + 0.61$$

These equations can be used to compute the rate of littoral drift along any beach by applying the longshore component of wave energy flux derived either from direct wave observations or hindcast from weather records.

TABLE OF CONTENTS

TABLE OF CONTENTS

(continued)

LIST OF TABLES

LIST OF FIGURES

LIST OF FIGURES

(continued)

NOTATION

Symbol	Explanation	Dimensions
B_t	Distance tracer centroid moved in time t	L
C	Celerity (wave phase velocity)	LT^{-1}
C	Concentration	
Cn	Wave group velocity	LT^{-1}
D	Mean grain diameter, phi units	$-Log_2$(diam. mm)
E	Electrical potential	(volts)
H	Wave height	L
I	Immersed weight transport rate	MLT^{-3}
J_x	Rate of diffusion	
KE	Kinetic energy	ML^2T^{-2}
L	Wave length	L
P	Incident wave energy flux	MLT^{-3}
P_a	Longshore component of wave energy flux	MLT^{-3}
PE	Potential energy	ML^2T^{-2}
Q	Volumetric transport rate	L^3T^{-1}
R	Electrical resistance	(ohms)
S	Unit length of wave crest	L
T	Wave Period	T
$\bar{V}$	Mean velocity of sand transport	LT^{-1}
W	Specific weight sea water	$ML^{-2}T^{-2}$
X	Unit length of beach	L

NOTATION

(continued)

Symbol	Explanation	Dimensions
y_b	Surf width	L
a	Pore space correction factor	
b	Subscript denoting wave break-point	
d	Turbulent diffusion coefficient	
g	Acceleration due to gravity	LT^{-2}
h	Water depth	L
k	Wave number $(2\pi/L)$	L^{-1}
o	Subscript denoting deep water	
t	Time	T
z	Thickness of mobile layer	L
rms	Subscript denoting root mean square wave height	
1/3	Subscript denoting "significant" wave parameters	
α	Angle of breaker incidence	degrees
ρ_s	Sediment density	ML^{-3}
ρ_w	Water density	ML^{-3}

I N T R O D U C T I O N

The extremely rapid development of our coastlines for both industrial and recreational use has produced the need for a variety of coastal engineering structures which alter the littoral drift system of a given locality to serve the local interests. Most of these structures are designed to reduce wave action or to decrease the rate of sand loss by littoral drift either for beach protection or to prevent harbor entrance shoaling. For instance, twin jetties at an inlet will stabilize the inlet to the depth required for navigation by constricting the flow so that the inlet will be at least partially self scouring, will reduce wave action in the inlet for navigation safety, and will trap littoral drift materials from the updrift direction which reduces shoaling.

If a total barrier to littoral drift such as inlet jetties is built, then the beaches on the downdrift side of the inlet will be starved by the amount of sediment trapped by the updrift jetty. In addition, accretion behind the updrift jetty will slowly extend the shoreline to the seaward end of the jetty, requiring that the jetty be lengthened if it is to continue to protect the inlet from shoaling. Erosion protection for the downdrift beaches may be necessary. This is often accomplished by placing all maintenance dredging spoil

from the channel on the eroding downdrift beaches, by installation of a permanent bypassing plant on the updrift side of the pass to continuously pump sand across the inlet to the downdrift side, by nourishing the downdrift beaches with sand from other sources, or by constructing unsightly groin fields or seawalls on the downdrift beaches.

Along sandy coasts of the United States, the rate of littoral drift is on the order of 200,000 to 1,000,000 cubic yards of sediment per year (Caldwell, 1966). Dams on our rivers are greatly reducing the sand supply available to our coasts, and the rapidly increasing number of coastal engineering structures are producing greater and greater disequilibrium of littoral drift systems with resultant beach erosion and harbor entrance shoaling. The severity of these problems will probably increase in the future as a result of further coastal development.

Any solution or alleviation of these problems requires a reliable predictive method for computing the rate of littoral drift in each direction at any proposed constuction site. As a result of war research during World War II and subsequent work (eg. Sverdrup and Munk, 1947), there are now wave forecasting relationships which apply weather data to forecast the height, period and angle of approach of waves to shorelines. Likewise these relationships can be used with long term weather records to hindcast waves for a locality and enable the researcher to predict statistically the local

wave regime. With the development of a good empirical relationship between the rate of littoral drift and wave characteristics such as height and angle of incidence, it will be possible to compute the rates of littoral drift along any shoreline. This will enable the engineer to design more efficient and hopefully less damaging structures and to predict prior to construction the effect of any structure on the local shoreline. In some cases, such prediction may be used to halt an entirely unfeasable project.

Since the late 1940's research has been directed toward developing a relationship to predict the rate of littoral drift. Putnam, Munk, and Traylor (1949) developed a relationship to predict the rate of longshore currents in the surf zone from knowledge of incident wave parameters. Application of this type of relationship to predict rates of sediment transport is difficult because of the variable width of the surf zone, and the fact that the longshore current is not directly responsible for the initiation of motion of all of the sediment that it carries. Turbulence associated with passing bores initiates most sediment motion. Once in motion, the sediment is transported by the longshore current until turbulence is reduced sufficiently for deposition to occur. The process repeats again with the next succeeding bore.

Watts (1953) studied the relationship between the rate of littoral drift to the south and the southward compon-

ent of wave energy flux at South Lake Worth Inlet, Florida. The rate of littoral drift was measured by collecting the spoil from a bypassing plant in a basin and surveying the basin to determine the volume of sand pumped (Fig. 1). Wave data was gathered from a pressure type wave gage and direction was measured by visual observations. This was a significant step. All of the problems of surf hydrodynamics, prediction of intermittant longshore currents and sediment suspension were ignored. The basic assumption was that the rate of littoral drift is proportional to the longshore component of wave energy flux, or power. In that study and subsequent studies this assumption has proven accurate to within the experiment error of the data gathered.

Additional data of this type was gathered near Anaheim Bay, California by Caldwell (1956). In his study the rate of littoral drift was determined by measuring the rates of erosion downdrift of a littoral drift barrier subsequent to a beach nourishment program. Using both the data from Watts (1953) and Caldwell (1956), Caldwell developed the following relationship between the longshore component of wave energy flux (P_a)(millions of ft-lbs/day/ft. beach) and the rate of littoral drift (Q)(cubic yards/day).

$$Q = 210\ P_a^{0.8} \qquad (1$$

A considerable number of laboratory data relating the rate of littoral drift to the longshore component of wave energy flux have been gathered both in this country and in

Figure 1

South Lake Worth Inlet and Bypassing Plant - The net littoral drift is to the south. The fixed dredge gathers littoral drift materials trapped by the updrift jetty and places this material on the downdrift side of the pass through the pipeline. Shoaling of the pass and bar development are reduced. The bypassed sand tends to nourish the downdrift beaches and reduces beach erosion. The retention basin shown was temporarily constructed to hold the pumped material to determine the rate of littoral drift to the south (Caldwell, 1956).

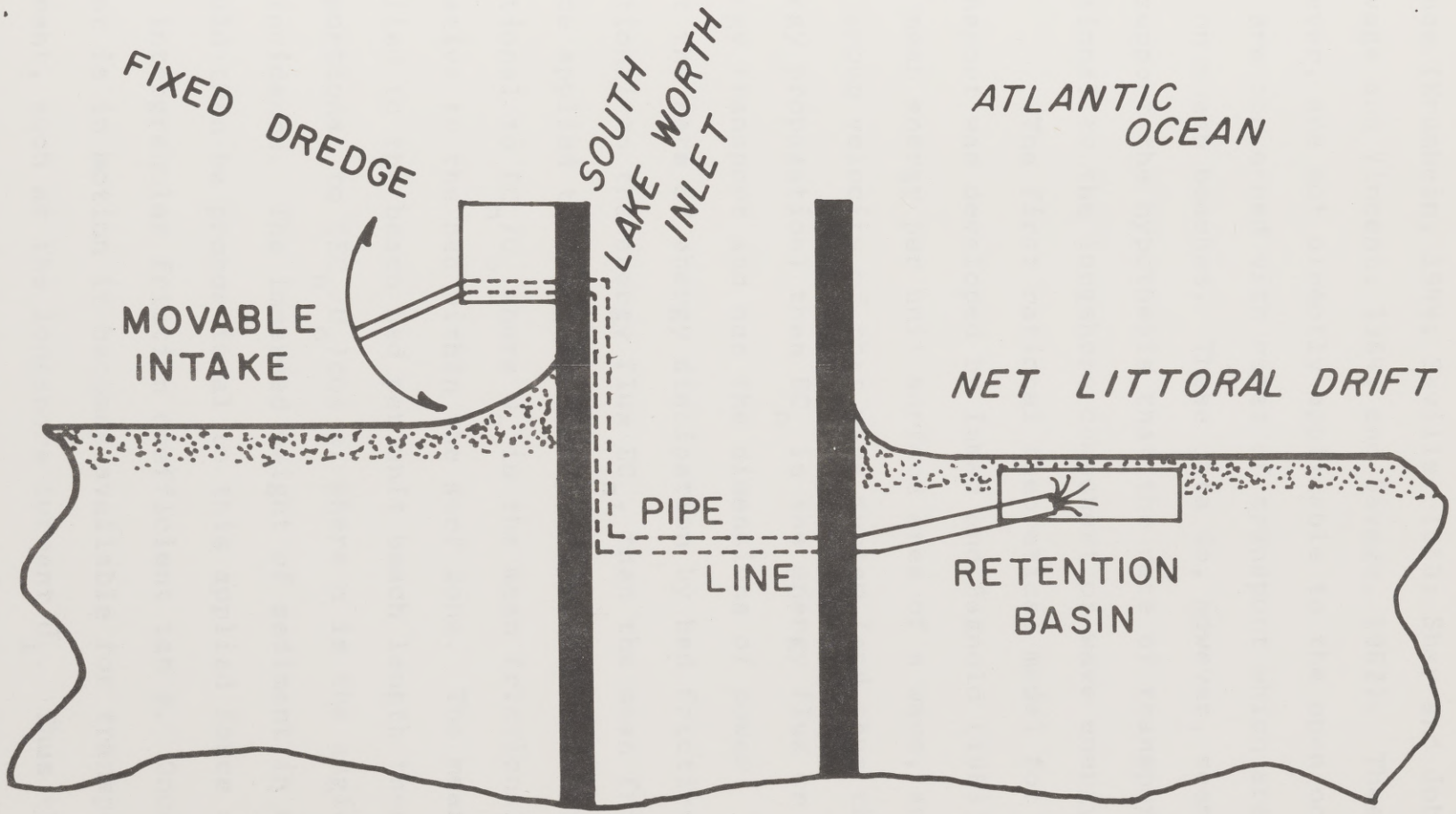

Figure 1

SOUTH LAKE WORTH INLET BYPASSING PLANT

France (Krumbein, 1944; Saville, 1950; Shay and Johnson, 1951; Sauvage and Vincent, 1954; and Savage, 1962). These data, however, are not directly applicable to the open ocean shores and are concerned with rates of transport which are negligible on ocean beaches. These data do, however, seem to roughly support the hypothesis that the rate of transport is proportional to the longshore component of wave energy flux.

The first rational theoretical model for longshore transport was developed by Inman and Bagnold (1963). If E is the mean energy per unit surface area of a wave, and C_n is the group velocity of that wave system (and thus the rate of energy propagation) then EC_n is the energy flux or rate of energy transport and has the dimensions of power. Assuming that the rate of energy dissipation by bed friction is proportional to the energy flux EC_n, then the mean frictional force applied to the beach bed per unit crest length is proportional to EC_n/U_o where U_o is the mean frictional velocity relative to the bed within the surf zone. The mean force applied to the beach bed per unit beach length then becomes proportional to $(EC_n/U_o)\cos \alpha$, where α is the angle of breaker incidence. The immersed weight of sediment in motion should than be proportional to this applied force divided by the intergranular friction coefficient $\tan \phi$. Once the sediment is in motion it becomes available for transport by any current, such as the longshore current $\bar{U}_l$. Thus the total immersed weight of sediment transported in unit time past a

section of beach becomes

$$I_l = K\frac{EC_n}{U_o}\frac{\cos\alpha}{\tan\phi}\bar{U}_l \qquad (2$$

where I_l is the immersed weight rate of sediment transport and K is a coefficient of proportionality.

The development of rapid and inexpensive methods of coating sand grains with fluorescent dyes enabled an entirely new approach to the study of sand movement by surf (Ingle, 1966). Through the use of these fluorescent tracers it is now possible to actually measure the rate of sediment transport in the surf for short time intervals. If the longshore component of incident wave energy flux can be measured for the same time period, then a relationship between the energy flux and sediment transport rate can be developed after a series of such measurements. The first such work was carried out by Komar and Inman for the Gulf of California and California coast beaches (Inman, Komar and Bowen, 1968; Komar, 1969; and Komar and Inman, 1970). Komar and Inman arrived at the following dimensionless relationship; $I = 0.77\ P\sin\alpha\cos\alpha$ where α is the angle of breaker incidence with the shoreline, I is the immersed weight transport rate, and P is the incident wave energy flux.

Until 1971, the validity of the assumption that the rate of littoral drift is proportional to the longshore component of wave energy flux had been supported only by an increasing body of experimental data gathered in the field and

laboratory. However, Komar (1971) demonstrated that the relationship is theoretically valid for two major types of longshore transport in the surf zone. It is theoretically valid for the special case of sawtooth transport in the swash zone and shallow surf zone where sand moves obliquely up the foreshore with the incoming wave swash and then returns normal to the shoreline with the backwash. The relationship is also valid for littoral transport by longshore currents in which the sediment is suspended by passing waves if the longshore current velocity is proportional to $U_m \sin\alpha$, where U_m is the orbital velocity under the breaking waves and alpha is the angle of incidence of the breakers with the shoreline.

Now that it seems evident that it is valid to relate the rate of littoral drift directly to the longshore component of wave energy flux, it is desireable to gather as much data as possible from many different types of shorelines in order to determine if there are other important variables which have not yet been considered. The Texas coast is wave dominated, with a tide range on only about 1.5 ft. and is characterized by extremely long barrier islands, deltaic headlands, and spits (Hayes, 1965). This shoreline is somewhat different from those studied by Watts, Caldwell, and Komar in that the offshore profile is very gentle, and the beach is multiply barred with 3 or more bars and troughs (Fig. 2). Furthermore the Mustang Island, Texas beaches where the data of this study were gathered are composed of

2.87 phi mean diameter sand which is considerably finer than the sand on any of the beaches of the other field studies. With the addition of the data from the 2.87 phi sands of the Texas beaches to the existing field data for 0.78, 1.32, and 2.5 phi size sands of the other field studies, it should be possible to determine if there is any detectable effect of mean grain diameter on the rate of littoral drift.

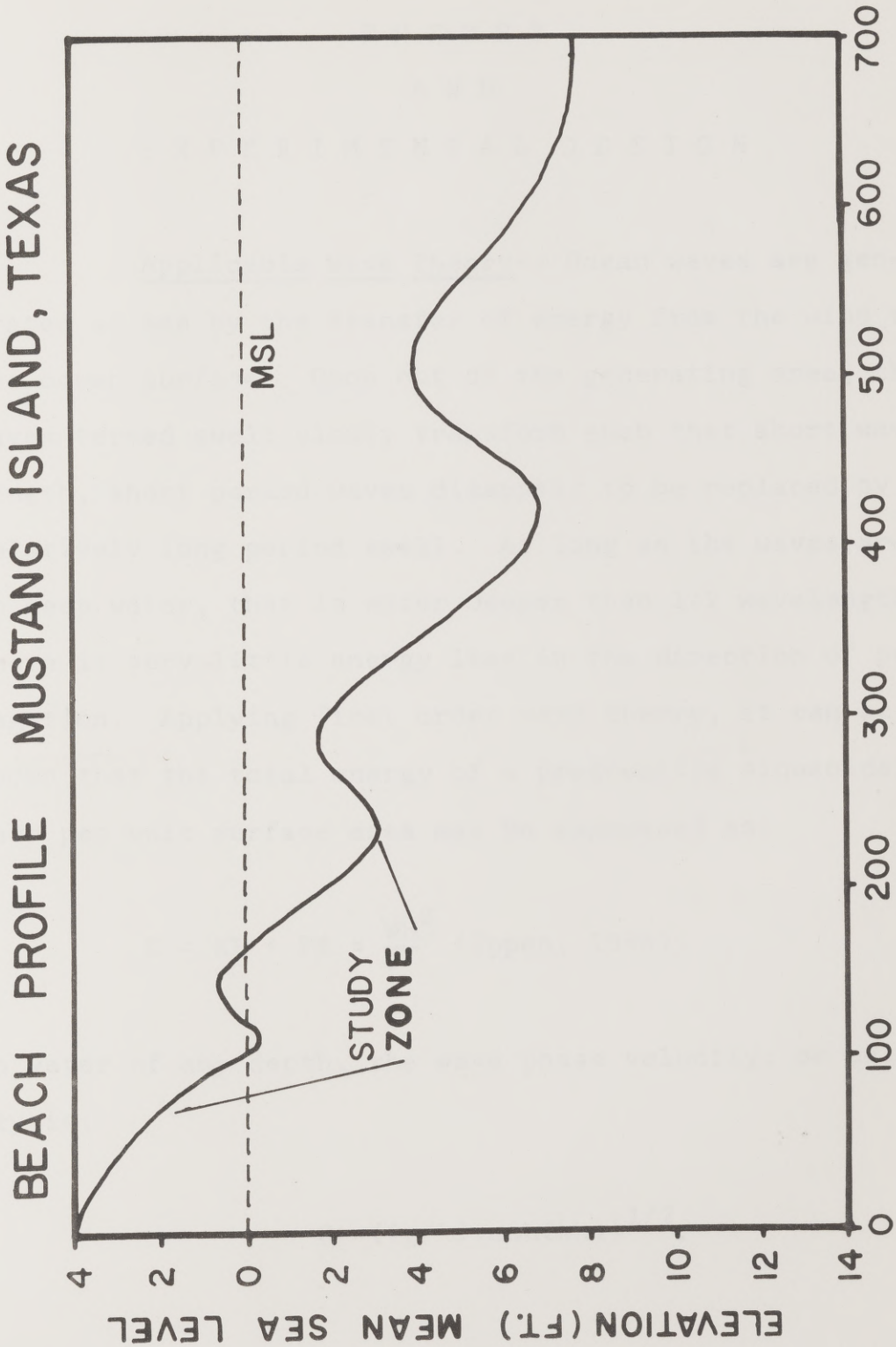

Figure 2

THEORY AND EXPERIMENTAL DESIGN

Applicable Wave Theory-- Ocean waves are generated at sea by the transfer of energy from the wind to the ocean surface. Once out of the generating area, the waves termed swell slowly transform such that short wavelength, short period waves disappear to be replaced by relatively long period swell. As long as the waves are in deep water, that is water deeper than 1/2 wavelength, there is very little energy loss in the direction of propagation. Applying first order wave theory, it can be shown that the total energy of a progressive sinusoidal wave per unit surface area may be expressed as:

$$E = KE + PE = \frac{WH^2}{8} \quad \text{(Ippen, 1966).} \qquad (3$$

In water of any depth, the wave phase velocity, or celerity is:

$$C = ((g/k)\tanh(kh))^{1/2}. \qquad (4$$

In deep water, the function (tanh(kh)) approaches 1 as a limit. Therefore, the deep water celerity reduces to:

$$C_o = (gL/2\pi)^{1/2} \quad (5$$

and for shallow water, the function (tanh(kh)) approaches kh as a limit rendering:

$$C = (gh)^{1/2}. \quad (6$$

We are interested in the rate of energy propagation, from deep water into shallow water and ultimately into the surf.

Since the rate of energy propagation of a wave group is equal to the group velocity, we must determine the group velocity for deep water and observe how it changes as the wave moves into shoal water. For any depth of water, the group velocity C_G can be expressed as follows:

$$C_G = Cn \quad \text{where} \quad (7$$

$$n = 1/2 \left(1 + \frac{2kh}{\sinh(2kh)} \right) \quad \text{and} \quad (8$$

$$k = 2\pi/L. \quad (9$$

Note that for deep water, the function sinh(2kh) approaches $e^{2kh}/2$ as a limit which is much greater than 2kh causing n to approach 1/2 as a limit. Therefore in deep water the group velocity is equal to one half of the celerity.
In shallow water the function sinh(2kh) approaches 2kh as a limit. Therefore, n approaches 1 as a limit and the group velocity and rate of energy propagation equal the shallow water celerity (Ippen, 1966).
As the wave moves into shallow water ($h<1/2$ L), the wave begins to feel bottom and the celerity is reduced (Fig. 3). There is little energy loss to bottom friction, and the energy is conserved by wave height (H) increasing. The result is that as the wave approaches the break-point where H is approximately equal to 0.78h, the wave is over-steepened such that the crest is high and sharp while the troughs are broad and flat. During the shoaling process, the wave celerity has been reduced to the group velocity, so that the rate of energy propagation is now the celerity.
So far, we are able to determine the energy flux P per unit wave crest length into the surf zone at angle α(Fig. 4). We wish to determine the longshore component of P, P_a per unit beach length. The relationship between the unit length of wave crest (S) and the unit length of beach (X) is $S = X\cos\alpha$, where α is the angle of breaker incidence (Fig. 5). Since the longshore component of wave energy

Figure 3

Definition Diagram for Oscillatory Waves

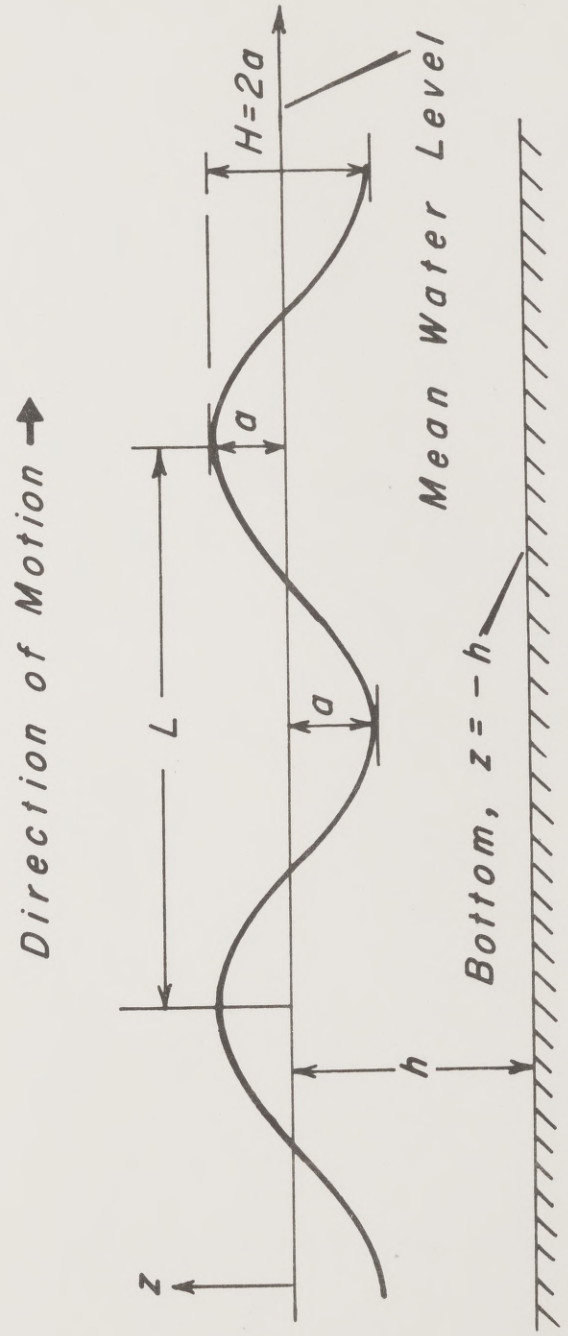

Figure 3

Figure 4

Generation of Littoral Drift by Waves

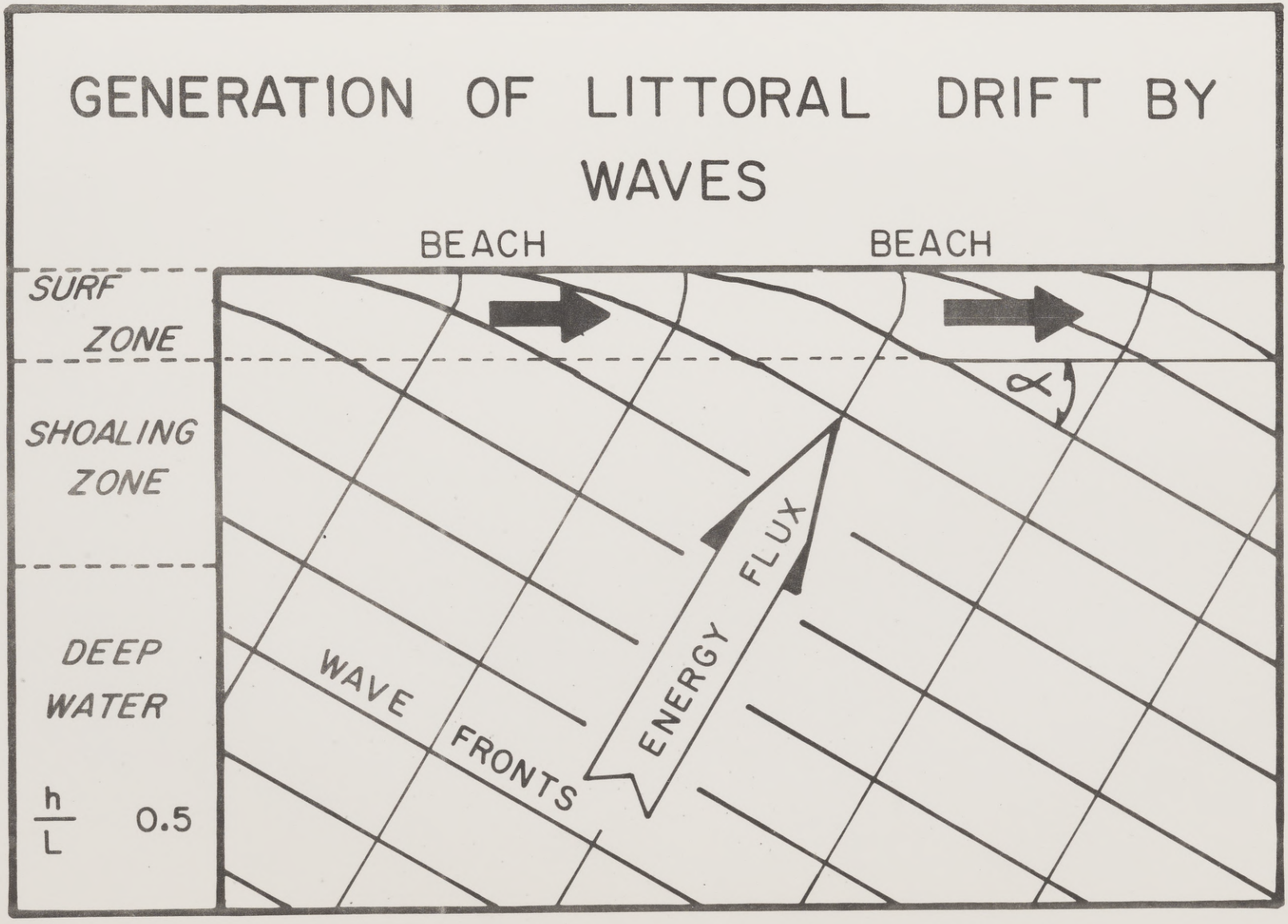

Figure 4

Figure 5

Vector Diagram

for

The Alongshore Component of Wave Energy Flux

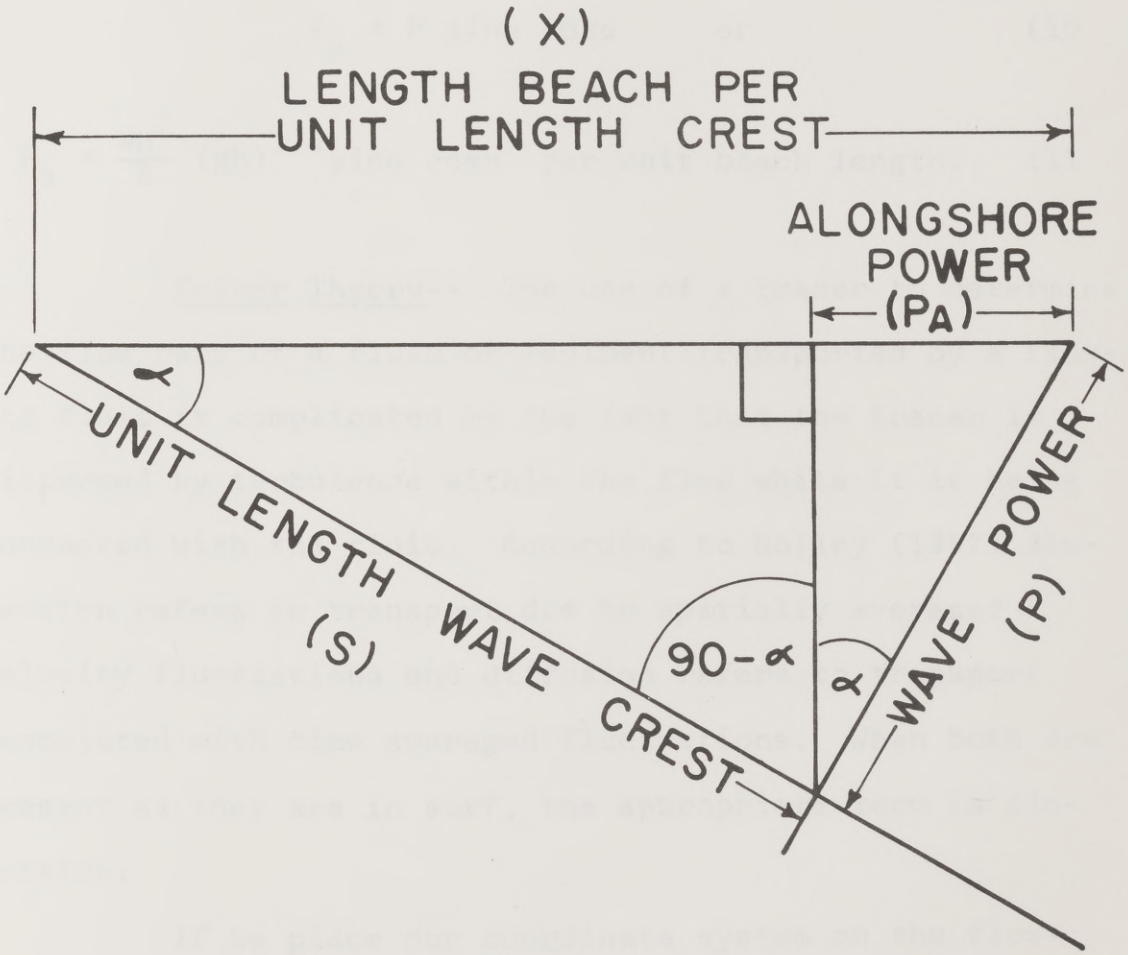

$$\frac{P_A}{\text{UNIT LENGTH BEACH}} = P \cos\alpha \sin\alpha$$

Figure 5

flux (P_a) is related to the incident energy flux (P) by the relationship $P_a = P \sin\alpha$, the longshore component of energy flux may be expressed as follows (after Caldwell, 1956; Ippen,1966):

$$P_a = P \sin\alpha \cos\alpha \quad \text{or} \quad (10$$

$$P_a = \frac{WH^2}{8} (gh)^{1/2} \sin\alpha \cos\alpha \text{ per unit beach length.} \quad (11$$

Tracer Theory-- The use of a tracer to determine the flow rate of a fluid or sediment transported by a flowing fluid is complicated by the fact that the tracer is dispersed by turbulence within the flow while it is being convected with the fluid. According to Holley (1967) dispersion refers to transport due to spatially averaged velocity fluctuations and diffusion refers to transport associated with time averaged fluctuations. When both are present as they are in surf, the appropriate term is dispersion.

If we place our coordinate system on the flowing fluid, we can examine the mathematics of turbulent dispersion without the slight complication of transport of the dispersing system. Dispersion is a process of concentration equalization, whereby one substance moves through another until a uniform distribution is achieved.

The rate of transport in some direction per unit area is proportional to the concentration gradient in that direction. This is an observed behavior, and the coefficient of dispersion must be determined in the laboratory or field. Fick's first law of diffusion (or dispersion) can be stated

$$J_x = - \frac{d\partial C}{\partial x} \qquad (12$$

where J_x is the rate of diffusion, d is the turbulent diffusion coefficient and $\partial C/\partial x$ is the concentration gradient in the x direction. The negative sign indicates that diffusion is into the region of decreasing concentration. Fick's second law expresses the rate of change of the concentration with time in terms of the spatial rate of change of the concentration gradient (Gebhard, 1968).

$$\frac{\partial C}{\partial t} = \frac{\partial (d\frac{\partial C}{\partial x})}{\partial x} \qquad (13$$

Thus if a starting set of concentrations throughout a fluid is well known and if the time and spatially averaged velocity fluctuations of the fluid in flow are well known, it will be possible to predict the concentration of the dispersing substance at any location and at any time with-

in the fluid. This information is totally lacking for fluid flow in the surf.

The purpose of the mathematical description of tracer mixing has been to demonstrate that the tracer will disperse as it is carried along with the sediment particles which it is tracing and that the rate of mixing is non-uniform and is dependent on both fluid properties and on the concentration gradient of the tracer itself. Our use of fluorescent marked sediment particles is simply to determine the flow velocity of the sediment in transport. According to Sheppard (1962), if the label and the fluid elements (unmarked grains) move together, the centroid of the label distribution will move with the mean velocity of the fluid (sediment in transport). Therefore, if we can determine the location of the tracer centroid at release time and its location at some subsequent time, then we can determine the distance traveled by the tracer during that time period, and thus the transport velocity of the tracer and the sediment. The centroid of the tracer at the time of release is simply the release location, or if two uniform releases are made, as in this study, it is midway between the two release locations.

After release, it is necessary to wait for a period of time for the sediment and tracer to be transported along the beach as littoral drift. Sampling must then

be carried out to determine the centroid of the tracer distribution and thus the distance that the sediment was transported. The following relationships will give the x and y coordinates of the centroid location for any sampling time (Fig. 6).

$$X = \frac{\sum_{y=0}^{y=b} \sum_{x=-\infty}^{x=\infty} XC_{(x,y)}}{\sum_{y=0}^{y=b} \sum_{x=-\infty}^{x=\infty} C_{(x,y)}} \qquad (14$$

$$Y = \frac{\sum_{y=0}^{y=b} \sum_{x=-\infty}^{x=\infty} YC_{(x,y)}}{\sum_{y=0}^{y=b} \sum_{x=-\infty}^{x=\infty} C_{(x,y)}} \qquad (15$$

where y is the onshore-offshore axis, x is the alongshore axis, y=0 is the edge of the swash zone, y=b is the breakpoint of the waves, and $C_{(x,y)}$ is the tracer concentration at location (x,y). The longshore distance that the tracer traveled since release is the x coordinate of the location of the tracer centroid at sampling time minus the x coordinate of the tracer release location.

$$B_t = X - x_r \qquad (16$$

where B_t is the distance traveled by the tracer in time t, X is the centroid coordinate in the longshore direction at time t, and x_r is the centroid location at release when time t=0. The mean velocity of sand transport is, then

Figure 6

Coordinate System

for

Tracer Centroid Computations


DISTANCE OFFSHORE (Y)
100
80
60
40
20
0
0
20
40
60
80
100
120
140
DISTANCE ALONGSHORE (X)
[C80,60]
C48,40

Figure 6

$$\bar{V} = B_t/t \qquad (17$$

where $\bar{V}$ is the mean velocity of sand transport. The volume rate of transport is given by the product of the flow velocity of the sediment ($\bar{V}$) and the cross section through which it is flowing. The cross section is bounded by the width of the surf zone (y_b) and the depth of the mobile layer (z). Therefore, the volume rate of flow (Q) is:

$$Q = \bar{V} y_b z. \qquad (18$$

Finally, the immersed weight rate of transport (I) is given by:

$$I = (\rho_s - \rho_w) agQ \qquad (19$$

where, ρ_s is the density of the sand, ρ_w is the fluid density, (a) is a pore space factor, taken to be equal to 0.65, and Q is the volumetric transport rate. It is preferable to use the immersed weight transport rate rather than the volume transport rate because it takes into consideration particle density (Komar, 1969) and is dimensionally consistent with the longshore component of wave energy flux with which it is to be compared (Inman and

Bagnold, 1963). This has the advantage that coefficients determined in one system of weights and measures will be directly applicable to other systems of weights and measures.

F I E L D

E X P E R I M E N T A L P R O C E D U R E

Wave Recording-- The experiments of this study were carried out on a beach with three or more bars offshore from and essentially parallel with the beach. Between each pair of bars there is a trough which is deeper than the bars on either side of it (Fig. 2). Under heavy surf conditions, the surf zone width may excede 2000 ft. At such times the bores of breaking waves may carry across most of the intervening troughs to the next inner bar obscuring the outline of the individual bars. However, under normal, moderate and light surf conditions when the surf zone is less than 1000 ft. wide, the bores of spilling waves quickly disappear in the troughs; and the waves are well reformed before breaking again on the following bar.

The wave gage used in this study is a simple single staff step resistance gage (Appendix I). The angle of breaker incidence was measured with a staff mounted hand bearing compass. Sights built into the mounting were aligned with the wave crest and the compass was read after the passage of the wave. Comparison of three pairs of bearings obtained with the staff mounted hand bearing

compass with accurate sextant measurements of those angles over a range of angles from $2^{\circ}30'$ to 83° showed a mean error of less than 30' for an angle measured by a pair of compass bearings. The angles and their individual errors were as follows: $30^{\circ}27'$, 33'; $83^{\circ}04'$, 04'; and $2^{\circ}30'$, 30'. The angle of incidence of the waves at the breakpoint can thus be measured to within the accuracy of the estimation of the shoreline azimuth at any given time. It is believed that the measurement of the angle of incidence of waves at the breakpoint is accurate to within one degree and that any inaccuracy is due to the variability of the incident wave direction and not due to the method of measurement.

In order to reduce the effect of variability of wave direction, experiments were conducted only on days with very simple incident wave trains. The following requirements were met for each experiment : 1) There was only one direction of wave approach; 2) If possible, the waves were residual swell from a storm which occurred several days prior to the experiment.

In all experiments the wave gage was placed just seaward of either the foreshore break-point or in the trough just seaward of the nearshore bar. As a result the waves measured had usually broken and reformed one or more times before measurement. All tracer experiments were

carried out in that portion of the surf zone shoreward of the wave gage. It would have been desireable to study the transport throughout the width of the surf zone, however, the limited manpower and equipment available coupled with the great width of surf zone on these nearly flat beaches precluded such a study (Fig. 2). It is believed that since the waves were measured seaward of the zone of transport studied and since they were measured before the final break that the calculated wave energies were those available to do the work of sediment transport and so the results are valid.

Wave Records and Data Reduction-- Each transport esperiment has a duration of about one hour. Just prior to release of the tracer sand updrift of the sampling grid, a wave record of about five minutes duration is taken. Similar wave records are made every 15 minutes until sampling time, and a final record is made just after sampling (Fig. 7). Thus the significant wave height used in the computation of wave energy flux is determined for a total record duration of 11 to 20 minutes encompassing the passage of over one hundred significant waves. Several times during each experiment, the angle of breaker incidence is measured at the breakpoint with the staff mounted hand bearing compass. Upon return to the laboratory a three to five minute segment of each wave record of the

Figure 7

Sample Wave Records

The wave height scale is for size reference only. The height of any individual wave is the difference between the height of its crest and its adjacent trough.

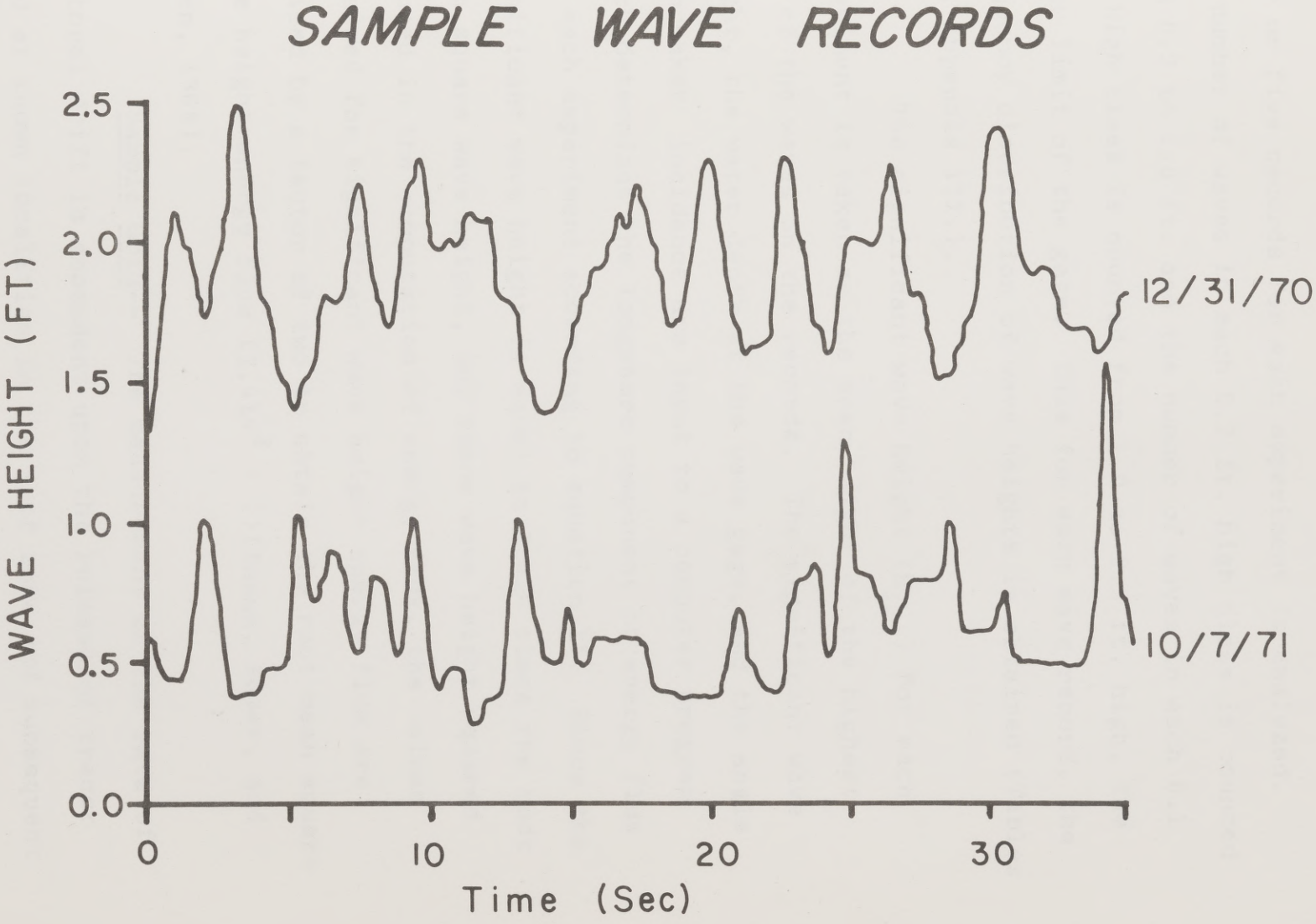
SAMPLE WAVE RECORDS
WAVE HEIGHT (FT)
2.5
2.0
1.5
1.0
0.5
0.0
0
10
20
30
Time (Sec)
12/31/70
10/7/71

Figure 7

four or five records for each experiment is analyzed. The number of waves in each 0.2 ft. high class is counted from 0.2 to 1.0 ft. and the number of waves in each 0.1 ft. high class is counted from 1.0 to 2.9 ft. high, the upper limit of the gage. Thus for each wave record, the frequency distribution of wave heights is obtained (Tables 3-9, Appendix III.).

The significant wave height ($H_{1/3}$) for each experiment is taken as the mean height of the highest 1/3 of the waves on the records. The significant wave height, the water depth at the wave gage, and the angle of breaker incidence are input to a computer program which determines the longshore component of energy flux for each experiment according to equation 11. Since the significant wave height is equal to 1.414 times the root mean square wave height, and since wave height squared is used in the computation of energy flux, the values obtained for significant wave height energy flux are divided by a factor of two to obtain the root mean square wave height energy flux ($1.414^2 = 2$)(Inman, Komar, and Bowen, 1968).

Sample Grid-- The measurement of the rate of littoral drift is dependent upon the release of tracer sand at known localities in the surf zone and subsequent sampling at known localities both updrift and downdrift

of the release position. In order to minimize error due to continued transport during sampling, it is desireable to use a grid system which will allow very rapid positioning within the sampling grid. Since there is a definite concentration gradient in the longshore direction such that there is a steep updrift gradient and a gentle tail of tracer concentration in the downdrift direction, a nonlinear longshore axis to the grid is desireable. Fewer samples are required where the concentration changes slowly with distance. Prior to release of the tracer, a double row of range poles is erected on the beach with spacing increasing in the downdrift direction. This enables the workers in the surf to rapidly station themselves along a range which is a known distance alongshore in the sampling grid (Fig. 8). Distance offshore is measured with a premarked rope with four equidistant markers for finding grid intersections. With this scheme a three man team can sample the entire grid of about 30 short cores in 10 minutes. Appendix IV contains the tracer concentration maps for each experiment. Note that the grid dimensions were varied in accordance with the approximate expected rate of littoral drift for each experiment. Two sets of data (not presented) were rejected because the sampling grid was too large for the very small transport that occurred in those experiments. A third data set (7/14/71) was rejected because the angle

Figure 8

Field Set-up

The wave gage sensor is located in the trough just seaward of the final breakpoint of the waves, with the wave gage recording equipment placed on the beach. The double row of range poles along the beach is used by the sampling crew to locate stations in the surf. Distance offshore is measured with a pre-marked rope.

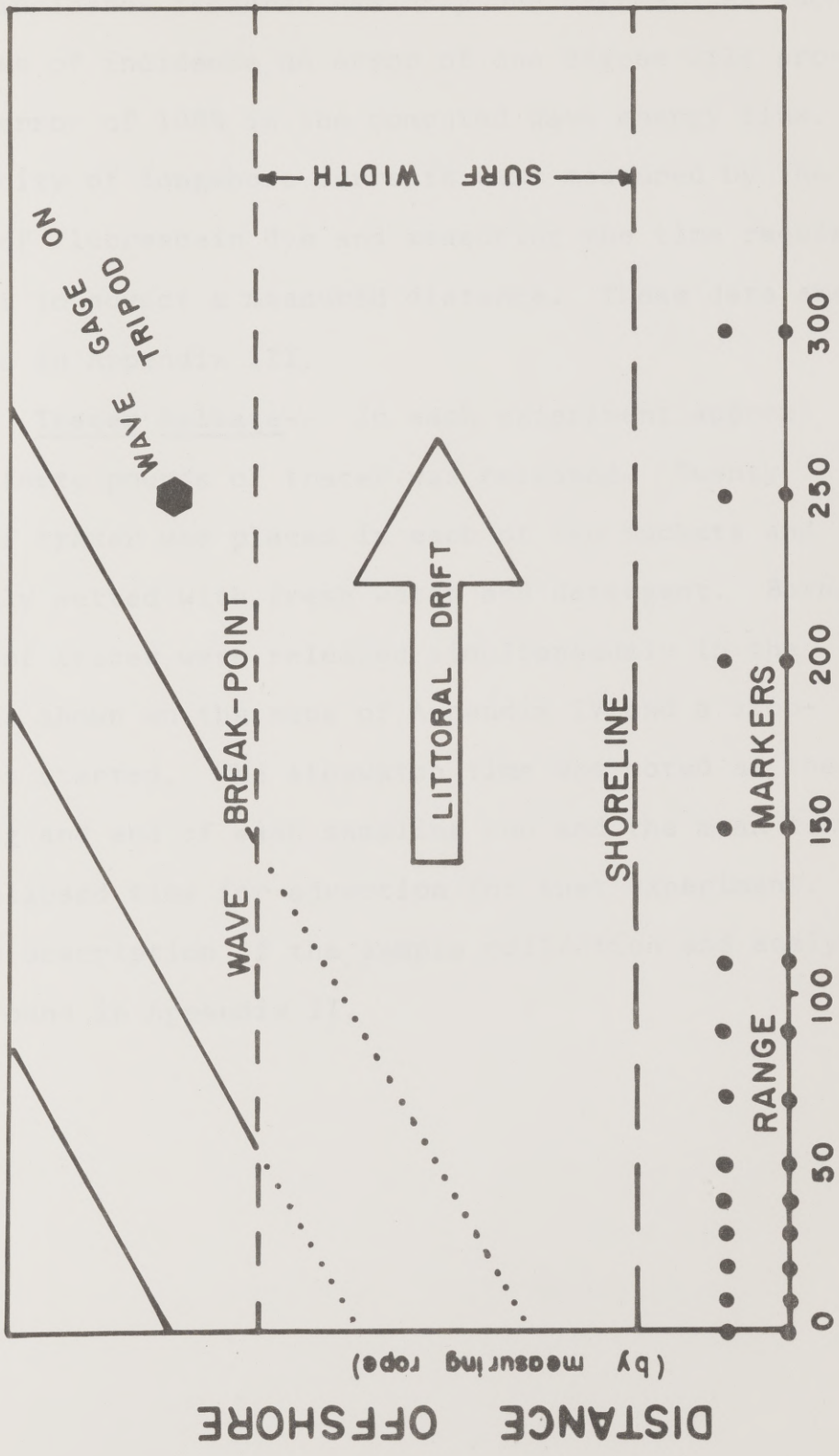
SURF WIDTH
WAVE GAGE ON TRIPOD
WAVE BREAK-POINT
LITTORAL DRIFT
SHORELINE
RANGE MARKERS
0
50
100
150
200
250
300
DISTANCE ALONGSHORE
DISTANCE OFFSHORE
(by measuring rope)

Figure 8

of wave incidence measured was only one degree. At such low angles of incidence an error of one degree will produce an error of 100% in the computed wave energy flux. The velocity of longshore currents were measured by the release of fluorescein dye and measuring the time required for it to advect a measured distance. These data are presented in Appendix III.

Tracer Release-- In each experiment approximately forty pounds of tracer was released. Twenty pounds of tracer was placed in each of two buckets and thoroughly wetted with fresh water and detergent. Both buckets of tracer were released simultaneously in the positions shown on the maps of Appendix IV and a stopwatch was started. The stopwatch time was noted at the beginning and end of each sampling run and the mean taken as the elapsed time for advection for that experiment. Detailed description of the sample collection and analysis can be found in Appendix II.

RESEARCH RESULTS

Presentation-- The results of the field experiments carried out in this study will be presented primarily as scatter plots of the longshore component of wave energy flux computed from wave data on the abscissa versus the corresponding immersed weight transport rate calculated from the tracer sand movement on the ordinate. The three existing sets of published field data will be included with the data gathered in this study, since no single data set is sufficiently extensive to represent a wide variety of beaches (Watts, 1953; Caldwell, 1956; and Komar, 1969). There is an abundance of laboratory data relating wave energy flux to longshore transport, but due to the very small size limitations to laboratory experiments, all of the data is clustered in a very low energy, low transport field (Krumbein, 1944; Saville, 1950; Shay and Johnson, 1951; Sauvage and Vincent, 1954; and Savage, 1962). Since these laboratory data are not directly applicable to the development of a useful relationship for the prediction of littoral drift on open ocean shores, and since there are adequate field data to accomplish this objective, the laboratory data are not included in this analysis.

All Field Data-- Figure 9 presents all of the available field data relating the longshore component of wave energy flux, hereafter termed power, to the immersed weight transport rate, hereafter termed transport. Considering that the accuracy of the computed longshore component of wave power depends on the accuracy of the measurement of the angle of breaker incidence, the possible error in this measurement estimated from comparisons with sextant angle measurements is shown in Figure 9 as horizontal lines representing the limits of wave powers computed from breaker angles one degree higher and one degree lower than those measured.

As one of the objectives of this study was to determine the effect of grain size on the rate of sediment transport, a least squares regression was computed for each of the individual sets of data of the same grain size (Fig. 9, Table 1). Prior to these computations, the data of Watson (this study) and that of Watts (1953) and Caldwell (1956) were all converted from wave power based on $H_{1/3}$ to wave power based on H_{rms} in order to compare with the data of Komar and Inman (1971) which is computed from the root mean square wave height. Examination of the data presented in Figure 9 shows no obvious effects of mean grain diameter on the rate of transport. All of the data regardless of mean grain diameter is closely grouped. However, the data

gathered in this study on Texas coast beaches shows a somewhat lower rate of transport for a given wave energy flux. Table 1 presents the results of computation of multiple regressions on each individual data set by grain size, and with the data sets combined with grain size factors included. Grain size is presented either in millimeters or phi units. F tests indicate that all regressions are significant at the 99 percent level of confidence. The percent of variability explained by the regression line computed for all data sets combined with grain size ignored is 76 percent. If grain size is included a regression is computed with a percent variability explained of 82 percent for grain size in phi and 81 percent for grain size in millimeters. There is, therefore, a five to six percent improvement in the variability explained by inclusion of a mean grain size term in the relationship between the longshore component of power and the immersed weight of transport.

The relationship determined for the rate of transport on the Texas coast is

$$\text{Log}_{10}(I) = 0.51\ \text{Log}_{10}(P_a) + 2.53 \qquad (20$$

while the relationship determined for all data sets

Figure 9

All Field Data

The data of Watson (this study), for 2.87 phi sand beaches, Caldwell (1956) and Watts (1953) for 1.32 phi sand beaches and Komar (1969) for 0.71 and 2.5 phi beaches are shown.


(⊙) Log10 (I) = 0.511 Log10 (PA) + 2.53
(⊕) Log10 (I) = 1.13 Log10 (PA) − 0.89
(X) Log10 (I) = 0.94 Log10 (PA) + 0.26
(Δ,●) Log10 (I) = 0.612 Log10 (PA) + 2.44
(All) Log10 (I) = 0.875 Log10 (PA) + 0.61
⊙ WATSON 2.87 φ
⊕ KOMAR EMB 0.71 φ
X KOMAR SSB 2.50 φ
Δ CALDWELL 1.32 φ
● WATTS 1.32 φ
8 Hrms
LOG10 (PA) ERG/(CM·Sec)
LOG10 (I) DYNE/Sec.
5
6
7
5
6
7

Figure 9

Table 1

Coefficients				Komar			Watts & Cald-well	% Var. Exp.	Wave Ht.
A	B	C	D	EMB	SSB	Watson			
0.943	0.00	0.00	0.264		x			97	rms
0.612	0.00	0.00	2.44				x	67	rms
0.511	0.00	0.00	2.53			x		92	rms
1.13	0.00	0.00	-0.893	x				91	rms
1.02	0.00	0.00	-0.243	x	x			94	rms
0.875	0.00	0.00	0.61	x	x	x	x	76	rms
0.804	0.00	-.207	1.36	x		x	x	84	rms
0.845	.903	0.00	0.42	x		x	x	82	rms
0.886	0.62	0.00	0.294	x	x	x	x	81	rms
0.862	0.00	-.145	0.92	x	x	x	x	82	rms
0.778	0.89	0.00	.754	x	x	x	x	73	Komar Hrms, Others, $H_{1/3}$

Explanation

Table 1 summarizes all of the multiple regressions computed on the field data. Columns A,B,C, and D are the coefficients presented in the equation below. The x's indicate which data sets are included. The column % Var. Exp. indicates the percent of the variability of the data explained by the regression equation. The equation relating the sediment transport rate to the longshore component of wave energy flux is:

$$\text{Log}_{10}(I) = A\ \text{Log}_{10}(P_a) + B(\text{size mm}) + C\ (\text{size } \phi) + D$$

combined and with grain size ignored is

$$\text{Log}_{10}(I) = 0.875\ \text{Log}_{10}(P_a) + 0.61 \qquad (21$$

and the relationship determined for all data sets with grain size in phi is

$$\text{Log}_{10}(I) = 0.86\ \text{Log}_{10}(P_a) - 0.145\ (\text{size}\ \phi) + 0.92\ . \qquad (22$$

Table 1 can be used to construct similar equations for all of the other data sets and for groups of those data sets.

Discussion-- The increase of five percent in the variability accounted for by inclusion of a grain size factor suggests that a refinement of the fundamental relationship between the longshore component of wave energy flux and immersed weight transport rate may be possible; but the data are inadequate to warrant such a refinement at this time. Relationships between other variables which are dependent on mean grain diameter should also be considered (Fig. 11). For example depth of disturbance of the sea bed in the surf zone increases with both increasing wave height and mean grain diameter (King, 1959). The explanation for greater depth of disturbance on coarser beaches is unknown, but may be due to the fact

that the mean diameter of the pore spaces will be larger in coarser sand (of the same sorting). Larger pore spaces may be able to transmit fluid forces deeper into the sediment and thus disturb the bottom to a greater depth.

It would appear that since the depth of disturbance or thickness of the mobile layer is one of the dimensions of the cross section through which the sand is flowing, increasing depth of disturbance for a given wave power will produce a greater transport rate. Thus it seems that coarser sand beaches may have higher transport rates than finer sand beaches for a given wave energy flux, because the depth of disturbance on coarser beaches is greater. However, coarser beaches generally form a steeper profile of equilibrium. Therefore, while the depth of disturbance is greater, the width of active surf is generally narrower, reducing another dimension of the cross section of sediment discharge. Increasing grain diameter and the narrowing of the surf zone due to increasing profile steepness result in a higher energy dissipation per unit area of bottom which favors increased transport. This, however, may be offset by the higher settling velocity of coarser grains and thus a shorter period of transport during the passage of each wave. Figure 10 graphically

Figure 10

Hypothetical Effect of Grain Size

on

Rate of Littoral Drift

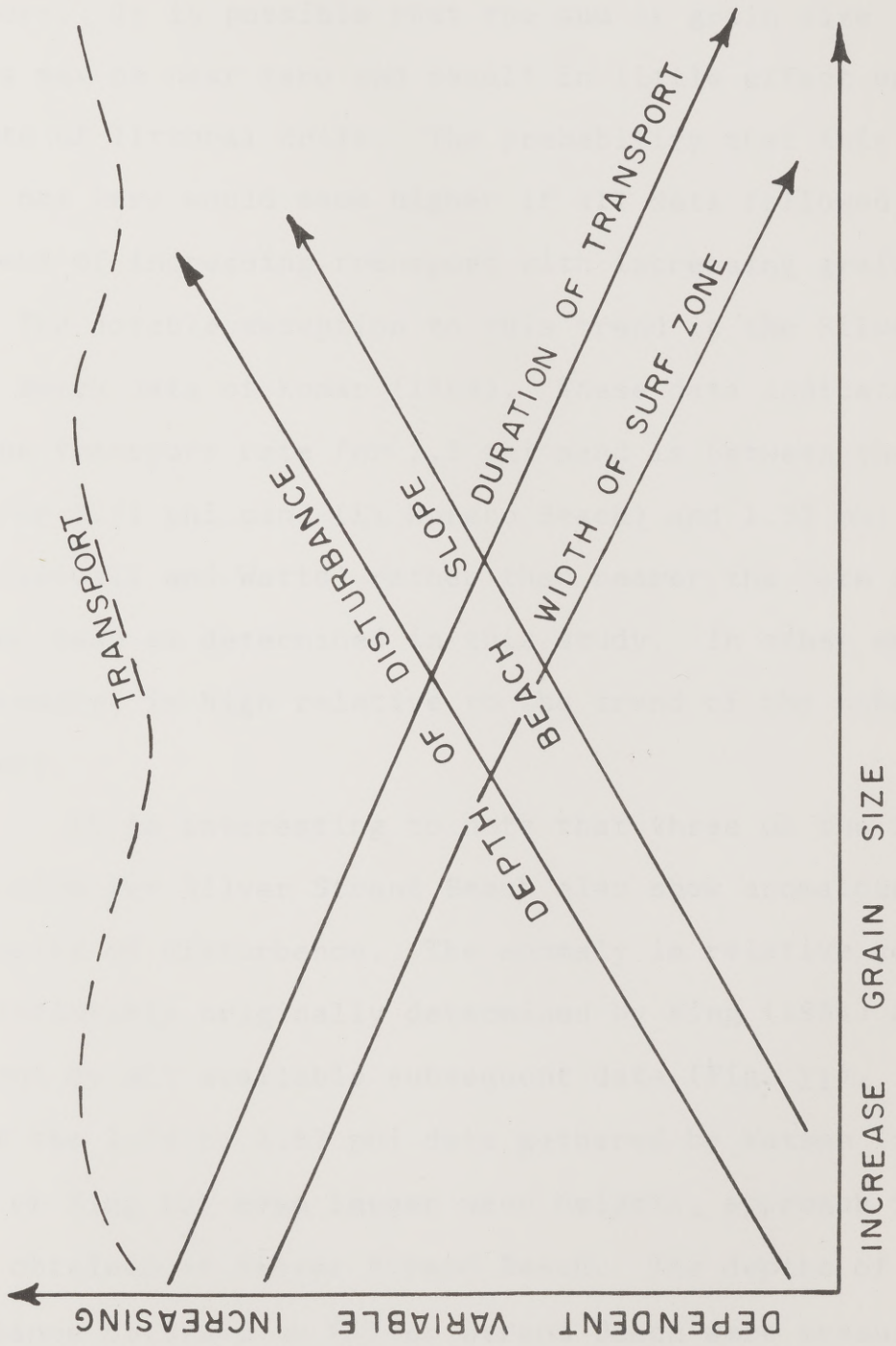
INCREASE GRAIN SIZE
DEPENDENT VARIABLE INCREASING
TRANSPORT
DISTURBANCE
SLOPE
DURATION OF TRANSPORT
DEPTH OF BEACH
WIDTH OF SURF ZONE

Figure 10

demonstrates the effect of each of these grain size dependent variables on the dependent variable, longshore transport. It is possible that the sum of grain size effects may be near zero and result in little effect on the rate of littoral drift. The probability that this sum is not zero would seem higher if all data followed the trend of increasing transport with increasing grain size. The notable exception to this trend is the Silver Strand Beach data of Komar (1969). These data indicate that the transport rate for 2.5 phi sand is between the rates for 0.71 phi sand (El Moreno Beach) and 1.32 phi sand (Caldwell and Watts) rather than nearer the rate for 2.87 phi sand as determined in this study. In other words the transport is high relative to the trend of the other data sets.

It is interesting to note that three of the four data points for Silver Strand Beach also show anomalously high depths of disturbance. The anomaly is relative to the relationship originally determined by King (1951) and supported by all available subsequent data (Fig. 11). None of the 1.78 to 2.87 phi data gathered by Watson (this study) or King for even larger wave heights, approach the values obtained at Silver Strand Beach. The depths of disturbance obtained on Silver Strand Beach were measured

Figure 11

Depth of Disturbance of Sand

in the Surf Zone

for Various Mean Grain Diameters

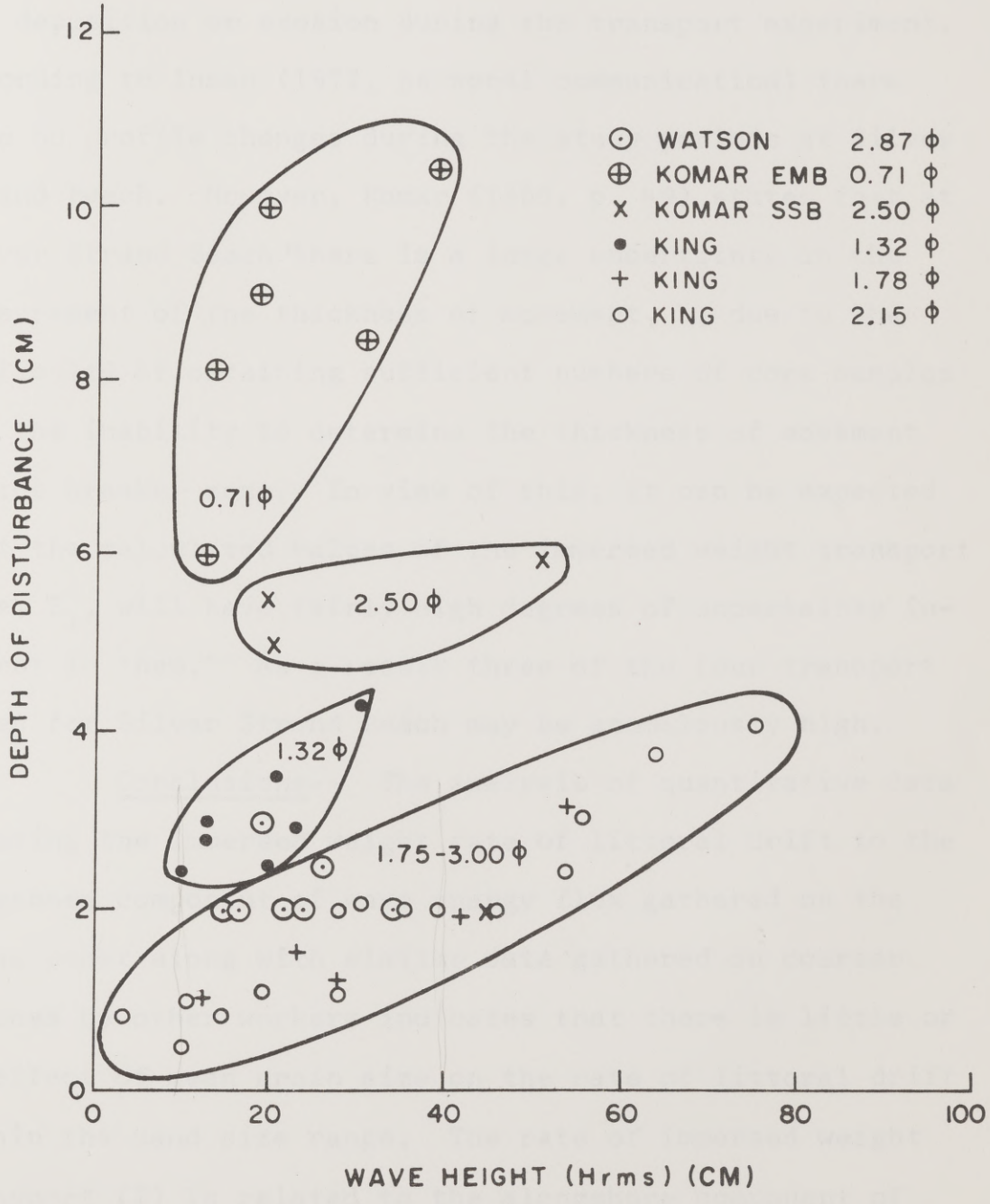
WATSON 2.87 ϕ
KOMAR EMB 0.71 ϕ
KOMAR SSB 2.50 ϕ
KING 1.32 ϕ
KING 1.78 ϕ
KING 2.15 ϕ
0.71ϕ
2.50ϕ
1.32ϕ
1.75-3.00ϕ
DEPTH OF DISTURBANCE (CM)
WAVE HEIGHT (Hrms) (CM)
0
2
4
6
8
10
12
0
20
40
60
80
100

Figure 11

by maximum depth of burial of the tracer sand in cores takin within the sampling grid, the same method as used in the present study. This method of determining the depth of disturbance will be reliable only if there is no net deposition or erosion during the transport experiment. According to Inman (1972, personal communication) there were no profile changes during the study periods at Silver Strand Beach. However, Komar (1969, p. 49) states that at Silver Strand Beach "there is a large uncertainty in the measurement of the thickness of movement, b, due to the difficulty of obtaining sufficient numbers of core samples and the inability to determine the thickness of movement in the breaker zone. In view of this, it can be expected that the calculated values of the immersed weight transport rate, S_1, will have fairly high degrees of uncertainty inherent in them." As a result three of the four transport rates for Silver Strand Beach may be anomalously high.

Conclusions-- The analysis of quantitative data relating the immersed weight rate of littoral drift to the longshore component of wave energy flux gathered on the Texas coast along with similar data gathered on coarser beaches by other workers indicates that there is little or no effect of mean grain size on the rate of littoral drift within the sand size range. The rate of immersed weight transport (I) is related to the alongshore component of

wave energy flux (P_a) by the following relationship for the Texas beaches studied.

$$\text{Log}_{10}(I) =).51\ \text{Log}_{10}(P_a) + 2.53$$

A more general relationship based on all existing field data (Watts, Caldwell, Komar and Inman, and this study) is as follows:

$$\text{Log}_{10}(I) = 0.875\ \text{Log}_{10}(P_a) + 0.61$$

To date, the field data are restricted to rather small wave heights and to sand sizes ranging from 0.71 phi to 2.87 phi. It would be desireable to extend the data into other sand sizes, however it is even more important that data be gathered under fully developed surf conditions. This has not yet been accomplished due to the logistical problems involved in attempting to gather quantitative data under heavy surf conditions. The present methods are wholly unsatisfactory for such conditions.

The U.S. Army Corps of Engineers Coastal Engineering Research Center has been working to develop a towed sensor to quantitatively trace concentrations of radioactive tracer sand (Duane and Judge, 1969). Such a machine could be operated in high surf, with the appropriate towing

vehicle or by being towed through the surf by cable from shore and a boat beyond the surf. If a method is devised to determine the depth of disturbance to use in conjunction with sediment transport velocities measured with this new instrument, it will be possible to measure accurately the rate of littoral drift under heavy surf conditions. Additional research should also be directed toward quantifying the relationship between depth of disturbance, grain size and wave height or energy. Transport velocity data gathered with the radioisotope method could then be used with predicted depth of disturbance and measured surf width to determine rates of littoral drift.

With the completion of these research objectives, we should have a truly general empirical relationship for the prediction of littoral drift on beaches regardless of grain size or surf intensity.

A P P E N D I X I

Design and Construction of a Portable Recording Wave Gage

Theory of Operation-- The series type step resistance wave gage operates on the principle of a circuit composed of a constant voltage direct current source, a variable resistance, and a load resistance all wired in series (Williams, 1969). As the resistance of the variable resistance is varied, the current through the load resistor varies (Fig. 12). The changing voltage across the load resistor can be monitored by a laboratory recorder to provide the basic elements of the wave gage. The variable resistor in the actual wave gage circuit consists of a series of fixed precision resistors. There is one resistor for each gage contact (Fig. 13). Note that as the gage contacts are shorted one by one to the movable contact from the bottom of the gage to the top of the gage, the total resistance of the resistor string is incrementally reduced, and thus the current through the load resistor is incrementally increased such that by Ohm's Law $E = IR$, the voltage drop across the load resistor is also incrementally increased and is recorded on the laboratory recorder connected across it. If the values of the resistors in the resistor string are such that

Figure 12

Series Circuit with Variable Resistor

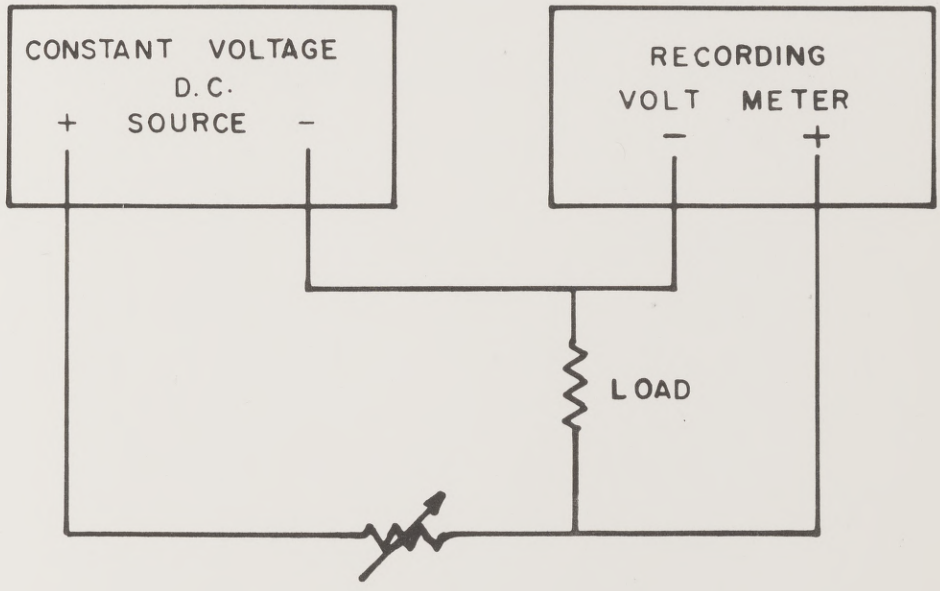

Figure 12

Figure 13

Simple Series Circuit

with a Chain of Resistors in

Series

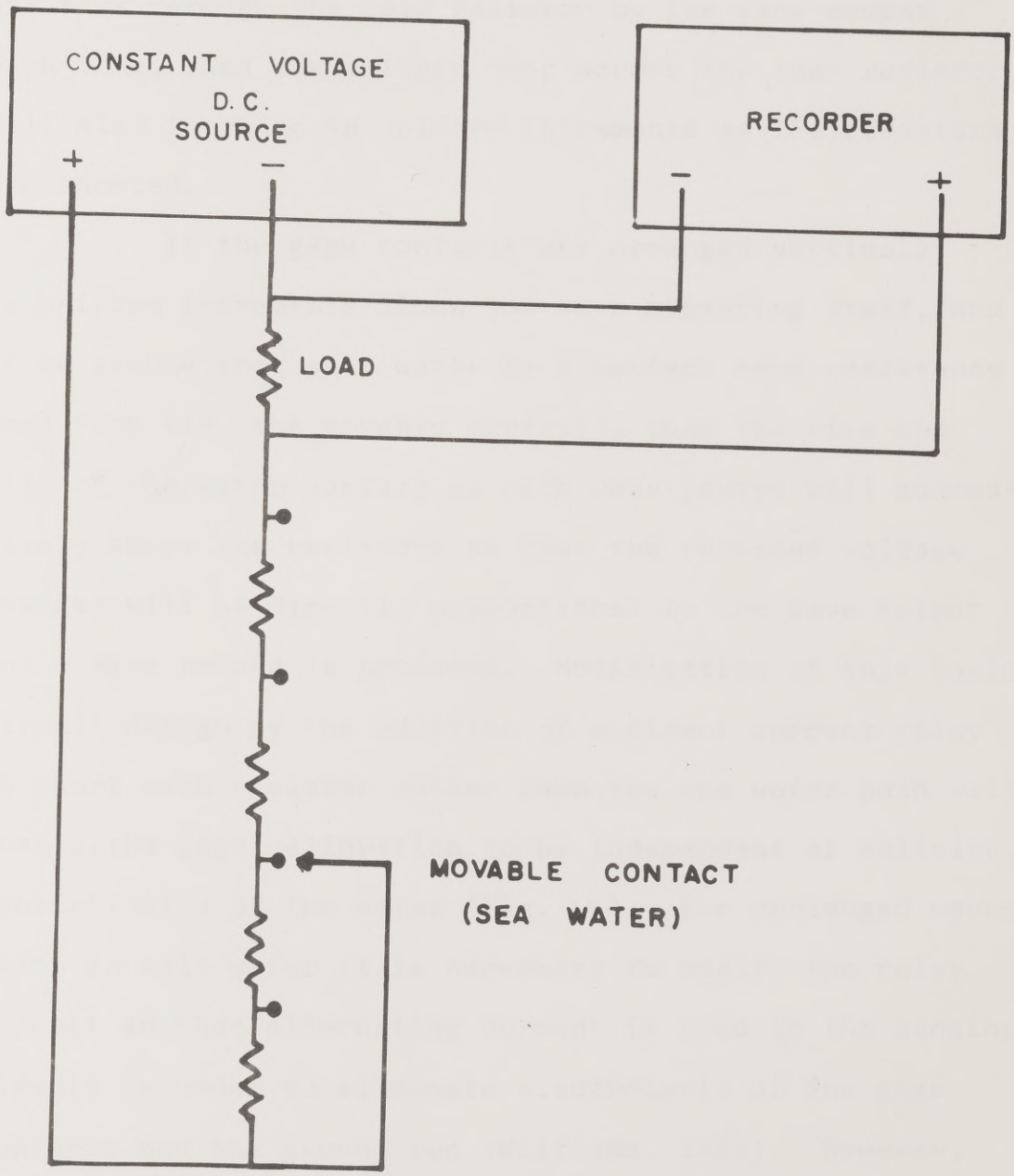
CONSTANT VOLTAGE
D.C.
SOURCE
+
−
RECORDER
−
+
LOAD
MOVABLE CONTACT
(SEA WATER)

Figure 13

removal of each successive resistor from the circuit by shorting raises the current through the entire circuit and thus through the load resistor by the same amount each time, then the voltage drop across the load resistor will also increase in uniform increments as the resistors are shorted.

If the gage contacts are arranged vertically at uniform increments along the wave measuring staff, and if we assume that salt water is a perfect zero resistance conductor (ie. the movable contact), then the rise and fall of the water surface as each wave passes will successively short the resistors so that the recorded voltage changes will be directly proportional to the wave height and a wave record is produced. Modification of this basic circuit design by the addition of a direct current relay to short each resistor rather than the sea water path will enable the gage calibration to be independent of salinity (resistivity) of the water (Fig. 14). For prolonged operation in salt water it is necessary to modify the relay circuit so that alternating current is used in the sensing circuit in order to eliminate electrolysis of the gage contacts and the ground rod (Williams, 1969). However, since this gage is intended for portable short term use and for minimum cost, electrolysis of the gage contacts will be negligible if the polarity of the gage contacts

Figure 14

Partial Wave Gage Circuit

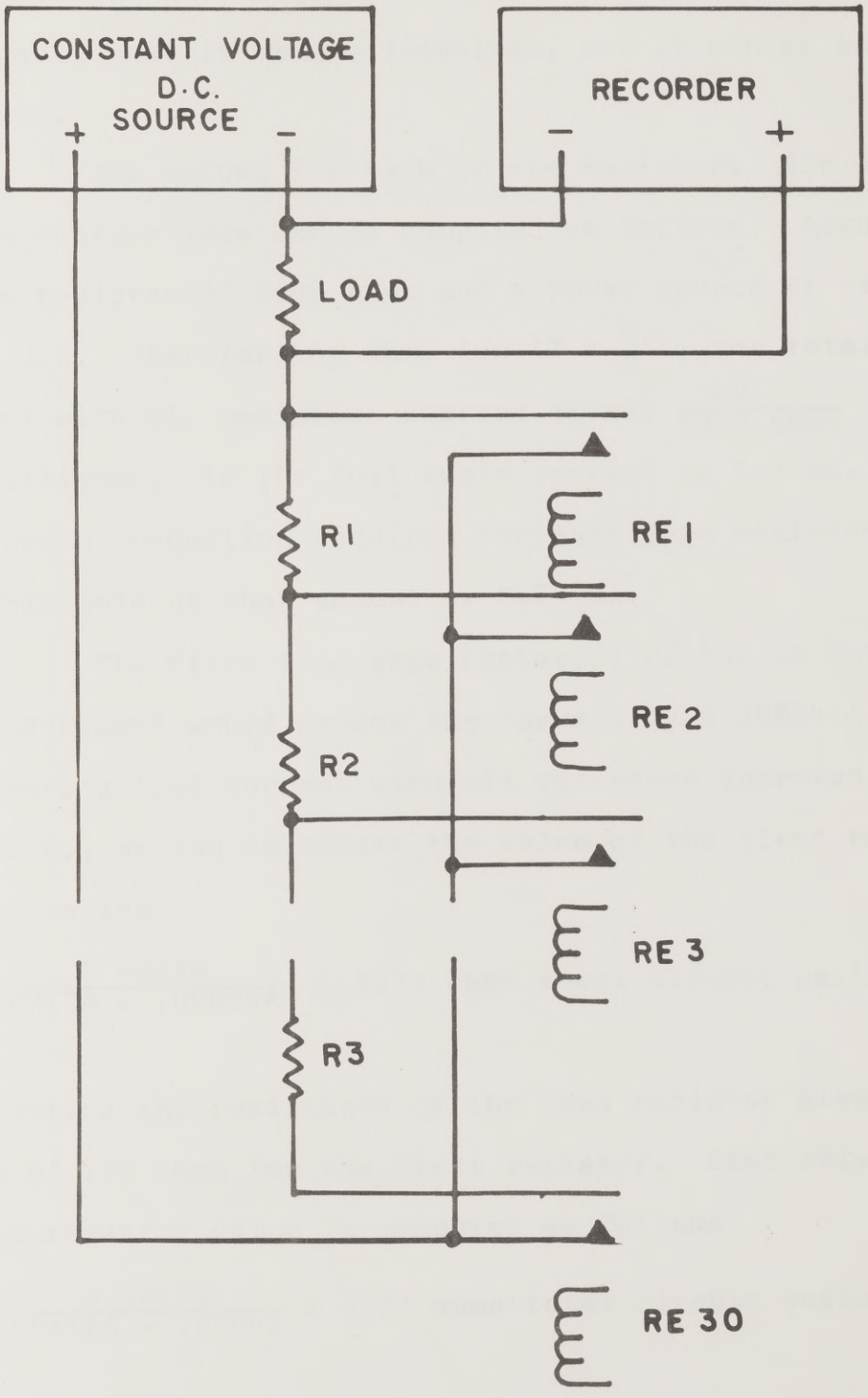
CONSTANT VOLTAGE
D.C.
SOURCE
+
−
RECORDER
−
+
LOAD
R1
RE 1
RE 2
R2
RE 3
R3
RE 30

Figure 14

is negative. This renders the ground rod positive with the result that it slowly dissolves, but it can be easily replaced.

The values for each of the resistors for a thirty contact gage can be computed as follows. Assume a load resistor of 5000 ohms and a power source of six volts d.c. Therefore by ohms law ($I = \frac{E}{R}$), the total current with all resistors shorted equals $\frac{6V}{5000 \text{ ohms}}$ or 1.2 milliamps. If the full scale current is 1.2 ma, then the current reduction required for each gage resistor is one thirtieth of that amount or 0.04 ma.

The first (top gage resistor) of the 30 intervals of measurement would reduce the current by 0.00004 A. Remembering that current with all resistors shoreted was 0.0012 A., we can calculate the value of the first resistor in the series.

$$\frac{6 \text{ volts}}{.0012A - .00004A} = 5172 \text{ ohms total circuit resistance.}$$

Subtracting the resistance of the load resistor gives a value of 172 ohms for the first resistor. Similarly, the second resistor value is computed as follows:

$$\frac{6 \text{ volts}}{.00116A - .0004A} = 5357 \text{ ohms total circuit resistance.}$$

Subtracting previous total resistance, 5357 ohms minus 5172 ohms is equal to 185 ohms, the value of the second

series resistor. All other resistors in the resistor string are computed in a similar manner (after Williams, 1969).

The complete circuit diagram of the 30 contact gage is presented in figure 15. The load resistor is replaced by a potentiometer (R30) to serve as a voltage divider to vary the output to the recorder and a second potentiometer (R31) serves as a calibration control to obtain linear response throughout the operation range. Switches S4 and S5 actuate the relays corresponding to contacts 19 and 29 respectively to be used in conjunction with the amplitude control R30 and the calibration control R31 to set the maximum amplitude on the strip chart recorder and to set the linearity. The recorder zero control is used to set the zero reading of the wave recorder. Table 2 is a list of the essential electrical components required to build the wave gage. A high resistance input voltage divider can be fabricated to step down the output of the wave gage to a more suitable value for the inputs of laboratory recorders if necessary. A suitable circuit is shown in figure 16.

Construction-- As shown in the circuit diagram, there are two circuit boards. A large circuit board holds all of the resistors and relays. This circuit board should be mounted in a waterproof box such as a large ammunition

Figure 15

Complete Circuit Diagram

for

Thirty Contact Step Resistance Relay

Wave Gage for Direct Current Operation

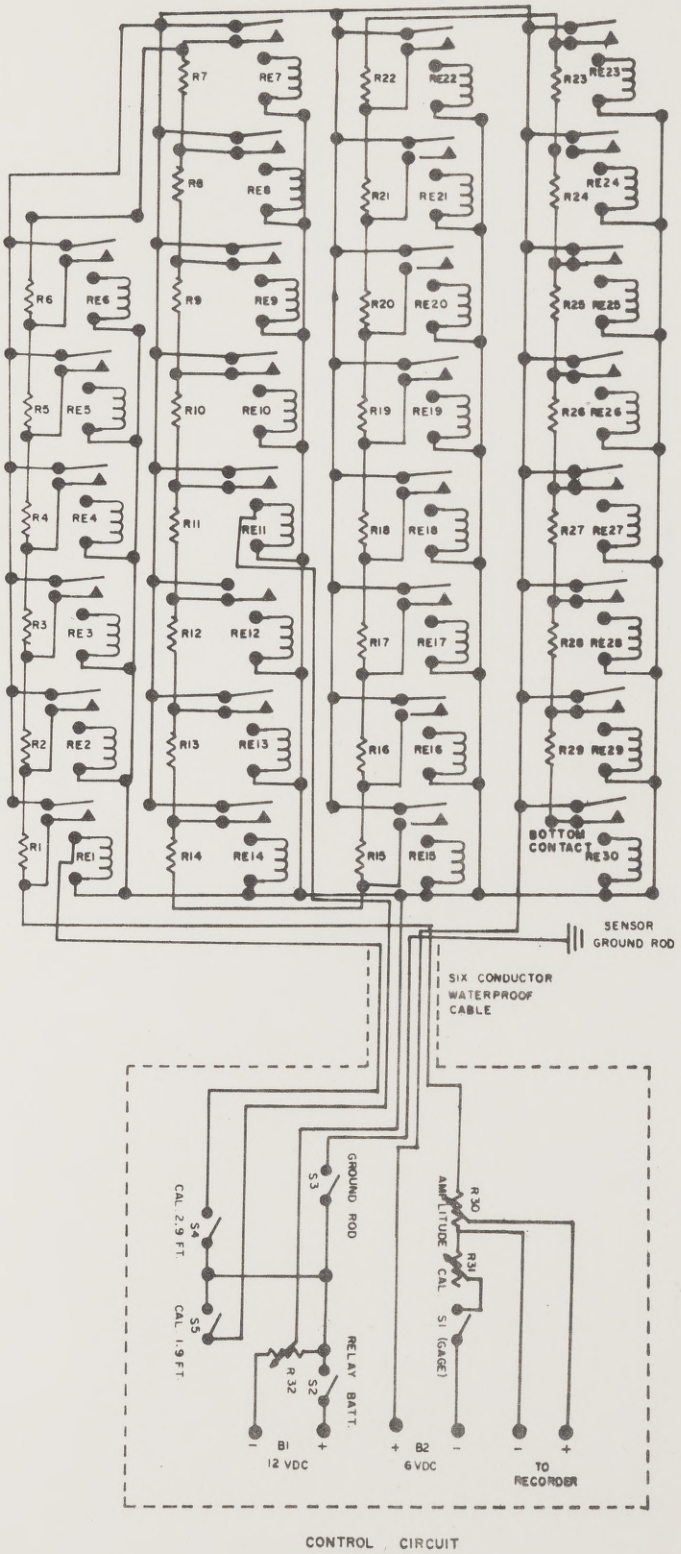

CONTROL CIRCUIT

Figure 15

Figure 16

Recorder Input Voltage Divider

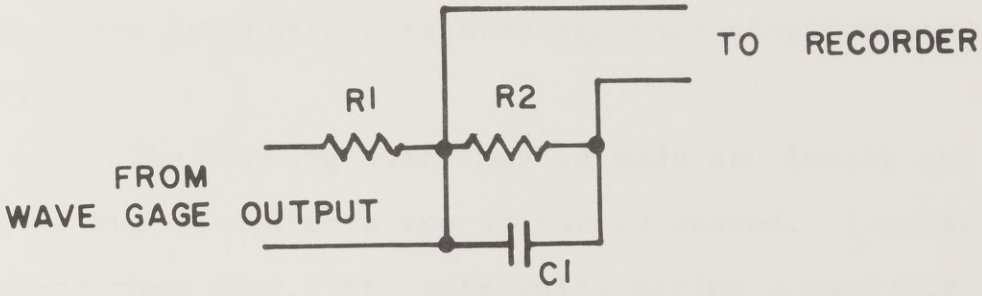

R1	10 MEGOHMS
R2	100K OHMS
C1	0.4 μf

Figure 16

box and attached to the sensing staff and the ground rod by a waterproof 32 to 36 conductor flexible cable. The smaller control circuit board and batteries must be located near the recorder and in a dry location either on a structure such as a pier or on shore. This control circuit is connected to the relay box by a waterproof six conductor cable of suitable length. It is advisable to use stranded wire throughout the construction as it is far less susceptible to breakage than single strand wire.

The sensing staff may be made any length as long as the 30 contacts are uniformly spaced. I chose to space them at 0.1 ft. intervals, making a gage 2.9 ft. long. Alternatively, the gage could be made shorter for use in laboratory waves or longer with a greater interval between the contacts for larger ocean waves. A suitable staff can be constructed by selecting a piece of PVC pipe of the appropriate length and mounting bronze machine screws for the gage contacts. Large holes can be drilled in the back side of the staff to access the bolts on the interior of the pipe to make the electrical connections to the 32 conductor cable. An extra contact serves for connection of the ground rod. After all conections are completed, the entire pipe can be filled with an insulator such as Devcon Flexane, a liquid rubber which sets at room

temperature. The ground rod should run parallel with the sensing staff and about one to two inches from the gage contacts.

Wave Gage Operation-- After the wave gage is set up it must be calibrated. After initial calibration, it should be necessary to check the calibration only with each future use as the instrument is stable as long as the six volt battery in the resistor circuit is in good condition. In order to calibrate the gage proceed as follows:

1. Turn on the recorder and switches S1 and S2.
2. Turn on switch S3 and adjust the voltage to the relays with control R32 until gage response to the waves is satisfactory.
3. Turn off the ground rod, switch S3 and turn on switch S4 which actuates the highest gage contact. Adjust the zero control for zero with S4 in the off position and adjust the amplitude control R30 for maximum scale reading of 29 divisions on the chart paper with S4 in the on position.
4. Switch off S4 and switch on S5. The pen should now show a scale reading of 19 divisions on the chart paper. If it does not come to the 19th division, then control R31

must be adjusted such that with S4 off and S5 on the pen is at the 19th division and with S4 on the pen is at the 29th division. It will be necessary to simultaneously adjust the amplitude control, R30, since the amplitude control and the calibration control interact. Once the instrument is adjusted by a series of successive approximations with the two controls, it is ready for use.

6. To place the gage in operation switch off S4 and S5 and reconnect the ground rod by turning on S3. Waves should now be recorded. After calibration, the amplitude control R30 can be adjusted without affecting the linearity of the calibration. It is suggested that the calibration control R31 be a screwdriver operated control so that is not accidentally adjusted.
7. Be sure to switch off the ground rod, S3, any time that the gage is not in operation in order to minimize electrolysis of the gage contacts.
8. A sample wave record is shown in figure 7.

TABLE 2

WAVE GAGE PARTS LIST

R1 172 ohms	R25 5000 ohms
R2 185	R26 7500
R3 199	R27 12500
R4 213	R28 25000
R5 231	R29 75000
R6 250	R30 4000 ohm pot
R7 272	R31 2500 ohm pot
R8 296	R32 200 ohm, 10W pot
R9 325	S1-S5 SPST toggle switches
R10 357	RE1-RE30 Magnecraft reed relays
R11 395	SPST normally off
R12 438	coil 6vdc.,200 ohm
R13 491	Magnecraft no. W102Mx-2
R14 551	B1 12 vdc storage battery
R15 625	B2 6vdc. lantern battery
R16 714	Recorder Heath EUW20-A or equivalent
R17 824	must have a mimimum chart speed of
R18 962	6 inches per minute
R19 1136	Power source for field operation of recorder
R20 1364	Heath MP-14 solid state inverter
R21 1667	
R22 2083	
R23 2679	
R24 3571	NOTE-- Resistors R1-R29 are 1% precision

A P P E N D I X II

Sand Dyeing and Tracing Apparatus

Methods for Fine Sand

General Requirements of a Tracer-- For any study in which a tracer is used to determine the characteristics of a transport system, the tracer behavior must closely apporximate the behavior of material in the system under study. Furthermore, the tracer must be easily distinguishable from the natural meterial. It is desireable that the tracer be inexpensive and easy to produce in large quantities.

At least four types of tracers have been used in sediment transport studies; irradiated natural sediment, natural sediments with color coatings, natural sediments with fluorescent coatings, and treated or untreated artificial sediments. In order to retain the same behavior as the sediment in the transport system under study, it is most desireable to mark sediment from that system for use as a tracer. The marking must have little or no effect on the hydraulic properties of the particles. Irradiation of the natural sediment and tracing with radiation counters achieves the desired hydraulic similarity. However, irradiation is expensive, slow, presents a possible health hazard, and may cause public

alarm. Use of simple color coatings is satisfactory for large particles, but unsatisfactory for very small particles since it is too difficult to distinguish them from unmarked particles when they are highly diluted with unmarked particles.

Application of fluorescent coatings to sediment from the system under study is highly satisfactory because tracing with the aid of ultraviolet light sources is inexpensive, there is no health hazard, and the marked grains can be readily distinguished even in very low concentrations. It is, however, difficult to coat fine sand grains with fluorescent coatings without severe aggregation. Some methods ignore aggregation during marking, and then granulate, sieve and reconstitute the dyed sand to the same grain size distribution as the prototype sediment (Teleki, 1966). This process is obviously tedious and very unwieldy for large volumes of tracer. Fine sand can be marked with anthracene, a water insoluble fluorescent organic compound by immersing the sand to be dyed in a chloroform solution of anthracene and then tumble drying it (Wright, 1962). The tracer produced in this manner shows very little aggregation, and fluoresces well under black light. The method is also inexpensive, and suitable for producing large volumes of tracer. Anthracene is, however, apparently susceptible to organic decay

under reducing conditions as it ceases to fluoresce when left in closed cores for a week or more. Therefore, if anthracene is used as a tracer, the samples must be either dried or analyzed immediately.

Yasso (1962) has developed methods of coating coarse sands and gravels with fluorescent coatings using Day-Glo paints along with various solvents and plastics for dilution and adhesion. Attempts to use the methods that Yasso developed with the fine 2.87 phi sands of the Texas Gulf Coast beaches resulted in excessive aggregation. The grains were, however, well-marked and highly visible. Another advantage of this system is the variety of colors which can be obtained by using the paints in the Day-Glo line. Because of these advantages I attempted to develop a marking method using Day-Glo paint systems which would not produce aggregates of fine sands.

Day-Glo Marking Method for Fine Sand-- Dilute 250 cc. of Day-Glo 202 line paint with four liters of benzene or toluene. Although this dilution is extreme, the coated grains are highly visible under ultraviolet light. Toluene is a much better solvent for the paint than benzene, but the benzene can be purchased very cheaply in bulk. Place about 25 to 30 pounds of clean dry sand in a tumbling drum such as a small cement mixer. Pour in the paint solution while tumbling until the sand

is thoroughly dampened, but not saturated. Tumble the sand until completely dry. There should be very little aggregation if the tumbling is continued until the sand is dry. This operation should be done out of doors since the solvents are both highly toxic and highly flammable.

Tracer Sampling Methods-- In any tracer sampling scheme it is necessary to either determine tracer concentration or a parameter related to tracer concentration. Tracer concentration is either determined at fixed locations as a function of time or at a fixed elapsed time as a function of location. In the case of tagged sediment particles, it is common to determine the number of tagged grains per unit area or per unit volume of the sediment at each sample location or sample time. A satisfactory method to determine tracer concentration per unit area for surficial grains is to press a vaseline coated card of known area on the sediment surface and count the number of marked grains on the card (Ingle, 1966). This method had a very serious drawback in that it gives no information about tracer distribution with depth in the sediment. Except in very unusual circumstances the sand transport will involve a variable thickness layer of sediment. Furthermore, transport within this layer will be faster at the top of the layer than down in the

bottom portions of it. For this reason, some workers have used bulk samples, taken either as grab samples with quantitative grab samplers (Komar, 1969) or short cores (Boon, 1969). The sample is then washed, dried and spread out on a large gridded table for counting the number of dyed grains. This however, does not give any information as to distribution with depth or maximum depth of transport and additional small diameter short cores have to be taken to determine depth of transport. Both of these bulk sampling methods are unsatisfactory for fine sand. It is very difficult and time consuming to wash, dry and spread out large bulk samples of fine sand and it is nearly impossible to count the marked grains in such large samples.

I have developed the following method to sample tracer concentration in fine sands. All tracer samples are taken in 3.5 cm. diameter polycarbonate core tubes. Each sample tube is about eight inches long and is equipped with a rubber stopper to seal each end of the tube. Both stoppers are removed and the core tube is pushed into the sediment by hand. After the tube penetrates about six inches, the top is stoppered so that the sand will be retained when the tube is withdrawn from the sediment. Immediately after withdrawal, the bottom

of the tube is stoppered, the upper stopper is removed and a small wash bottle is used to suck all of the water off of the top of the sediment in the sample tube. If the core tubes are then kept vertical, there will be very little mixing of the sand in the core and the tracer distribution in the sample tube will be a good representation of the tracer distribution at the site sampled. Three people can sample at a rate of about two cores per minute with this method.

The sample cores are kept in vertical storage and are kept stoppered so that they will not dry out until they are counted in the laboratory. Each core is then placed in a device to extrude it from the core tube in a controlled fashion (Fig. 17). The number of marked grains on the surface of the core is counted, and then the core is extruded and sliced off, one half centimeter at a time and the number of grains on each of these surfaces is counted. This procedure produces a representation of the total number of dyed grains per unit surface area of the site sampled, the distribution of tracer with depth, and the maximum depth of transport for the entire area under study. Advantages of this tracer sampling method for fine sands include rapid sampling time, good control of tracer distribution with depth at each sample location within the grid, and mimimum preparation time.

Figure 17

Precision Core Extruder

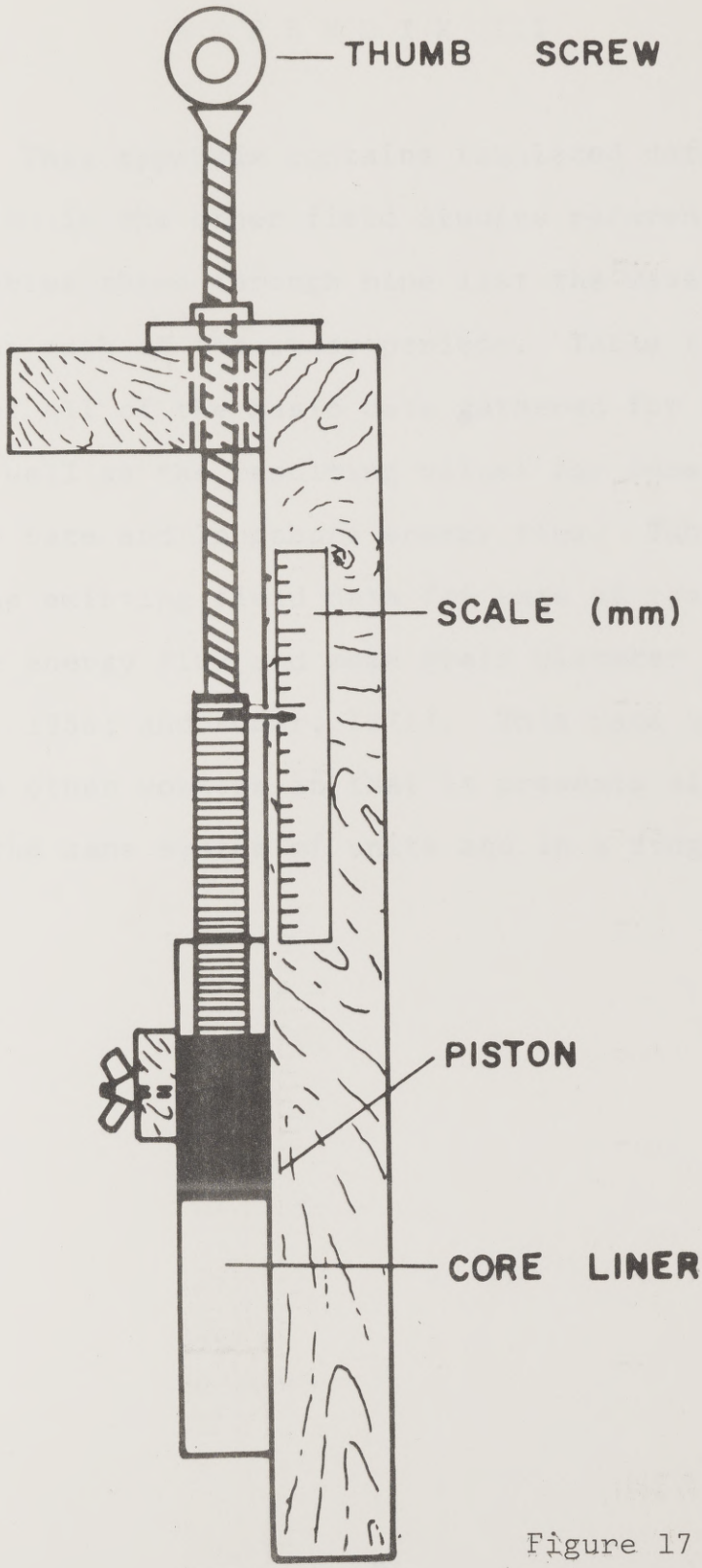

Figure 17

A P P E N D I X III

This appendix contains tabulated data gathered in this and in the other field studies referenced in the text. Tables three through nine list the wave characteristics for each of the study periods. Table ten is a summary of all of the basic data gathered for each experiment as well as the resulting values for immersed weight transport rate and longshore energy flux. Table 11 lists all of the existing field data for rate of transport, longshore energy flux and mean grain diameter (Watts, 1953; Caldwell, 1956; and Komar, 1971). This data may prove useful to other workers in that it presents all known field data in the same system of units and in a single location.

TABLE 3

Wave Data 12/31/70

Height (ft)	Frequency #waves	Duration (sec)	$T_{1/3}$ (sec)	$H_{1/3}$ (ft)	H_{rms} (ft)
0.2	53	630	8.3	1.2	.85
0.4	33				
0.6	37				
0.8	39				
0.9	19				
1.0	13				
1.1	12				
1.2	17				
1.3	8				
1.4	4				
1.5	0				
1.6	1				
1.7	1				
1.8	1				

TABLE 4

Wave Data 3/17/71

Height (ft)	Frequency # waves	Duration (sec)	$T_{1/3}$ (sec)	$H_{1/3}$ (ft)	H_{rms} (ft)
0.2	26	630	9.3	1.6	1.1
0.4	28				
0.6	23				
0.8	21				
0.9	14				
1.0	9				
1.1	12				
1.2	11				
1.3	7				
1.4	15				
1,5	8				
1.6	12				
1,7	6				
1.8	4				
1.9	3				
2.0	5				
2.1	1				
2.2	3				
2.3	3				
2.4	1				
2.5	1				
2.6	1				
2.7	2				

TABLE 5

Wave Data 4/7/71

Height (ft)	Frequency # waves	Duration (sec)	$T_{1/3}$ (sec)	$H_{1/3}$ (ft)	H_{rms} (ft)
0.2	50	930	5.1	1.1	0.78
0.4	83				
0.6	94				
0.8	82				
0.9	34				
1.0	16				
1.1	12				
1.2	9				
1.3	8				
1.4	5				
1.5	4				
1.6	4				
1.7	3				
1.8	2				
1.9	3				

TABLE 6

Wave Data 7/14/71

Height (ft)	Frequency # waves	Duration (sec)	$T_{1/3}$ (sec)	$H_{1/3}$ (ft)	H_{rms} (ft)
0.2	109	1260	7.1	1.0	0.71
0.4	200				
0.6	154				
0.8	74				
0.9	42				
1.0	22				
1.1	14				
1.2	8				
1.3	7				
1.4	3				
1.5	6				
1.6	1				
1.7	1				

TABLE 7

Wave Data 8/16/71

Height (ft)	Frequency # waves	Duration (sec)	$T_{1/3}$ (sec)	$H_{1/3}$ (ft)	H_{rms} (ft)
0.2	62	750	5.9	0.9	0.64
0.4	116				
0.6	110				
0.8	78				
0.9	23				
1.0	12				
1.1	7				
1.2	2				
1.3	1				
1.4	2				
1.5	1				
1.6	0				
1.7	1				

TABLE 8

Wave Data 9/7/71

Height (ft)	Frequency # waves	Duration (sec)	$T_{1/3}$ (sec)	$H_{1/3}$ (ft)	H_{rms} (ft)
0.2	92	805	4.3	0.7	0.5
0.4	215				
0.6	126				
0.8	46				
0.9	10				
1.0	4				
1.1	1				
1.2	1				
1.3	0				
1.4	1				

TABLE 9

Wave Data 10/7/71

Height (ft)	Frequency # waves	Duration (sec)	$T_{1/3}$ (sec)	$H_{1/3}$ (ft)	H_{rms} (ft)
0.2	148	720	6.3	0.8	0.57
0.4	118				
0.6	63				
0.8	27				
0.9	13				
1.0	7				
1.1	2				
1.2	1				
1.3	0				
1.4	1				

TABLE 10

BASIC DATA FOR EACH EXPERIMENT

Date	12/31/70	3/17/71	4/7/71	8/16/71	9/7/71	10/7/71
P_a (H_{rms}) (ft-lb/sec-ft)	11.8	6.4	6.8	3.9	2.2	0.98
P_a (H_{rms}) (erg/sec-cm)	5.2×10^6	2.8×10^6	3.0×10^6	1.7×10^6	9.5×10^5	4.3×10^5
I (lbs/sec)	2.13	1.48	1.28	1.21	1.06	0.50
I (dynes/sec)	9.5×10^5	6.6×10^5	5.7×10^5	5.38×10^5	4.7×10^5	2.24×10^5
Depth Disturb. (cm)	2.5	2.0	2.0	3.0	2.0	2.0
Surf Width (ft)	130	110	130	50	40	55
Ang. Incidence	12°	4°	8°	8°	6°	3°
$H_{1/3}$ (ft)	1.2	1.6	1.1	0.9	0.7	0.8
H_{rms} (ft)	0.85	1.13	0.78	0.64	0.49	0.57
Wave Gage Depth	3.2	2.5	3.3	2.3	3.6	1.7
Period $T_{1/3}$ (sec)	8.3	9.3	5.1	5.9	4.3	6.3
Centroid Velocity (cm/sec)	.101	.110	.076	.206	.22	.070
% Tracer Recovery						
By computation	90	48	22	43	23	23
By count	240	96	44	87	47	46
Grain diam. (phi)	2.87	2.87	2.87	2.87	2.87	2.87

TABLE 11

LITTORAL DRIFT DATA

Source	$Log_{10}(I)$ Dynes/sec	$Log_{10}(P_a)$ Erg/cm-sec	Size mm	Size phi
	5.98	6.72	0.137	2.87
	5.82	6.45	"	"
	5.76	6.48	"	"
Watson	5.73	6.23	"	"
	5.67	5.98	"	"
	5.35	5.63	"	"
	6.65	6.63	0.6	0.71
	6.93	7.02	"	"
	6.41	6.48	"	"
	6.00	6.18	"	"
Komar	6.16	6.30	"	"
(Emb)	6.63	6.58	"	"
	5.79	5.78	"	"
	5.95	6.26	"	"
	5.46	5.78	"	"
	6.32	6.26	"	"
	6.11	6.18	0.175	2.5
Komar	7.48	7.58	"	"
(Ssb)	6.67	6.96	"	"
	6.58	6.61	"	"
	7.02	7.20	0.4	1.32
	7.28	7.66	"	"
Caldwell	6.43	6.79	"	"
	6.74	7.51	"	"
	7.17	7.44	"	"
	6.88	6.64	"	"
	6.80	6.97	0.4	1.32
	6.48	6.96	"	"
	6.55	6.67	"	"
	7.06	7.06	"	"
	6.40	6.46	"	"
Watts	6.56	7.07	"	"
	6.48	6.81	"	"
	6.47	6.62	"	"
	6.13	6.05	"	"
	6.31	6.57	"	"
	6.31	6.01	"	"
	6.09	6.33	"	"

A P P E N D I X IV

TRACER MAPS

This appendix contains a map of the tracer distribution at sampling time for each of the data sets. The solid black circles represent the tracer release locations. The circles with the dot in the center are sampling stations. The black X denotes the location of the tracer centroid at the time of sampling. At the time of release, the tracer centroid is located midway between the two release points. The tracer distribution at the time of sampling is contoured on an arbitrary concentration parameter. For each study date there is a map of tracer concentrations determined by the core sampling and analysis method described in Appendix II. In addition, the greased card method of sampling was also used on December 12, 1970 and on March 3, 1971. These two maps have the notation "cards" on them. All of the maps show a strong concentration gradient on the up-current side with a long tail in the downdrift direction with the exception of the map for July 7, 1971. This data was gathered under conditions of almost no littoral drift so that the concentration map shows near equal dispersion in all directions with no dominant direction of transport.

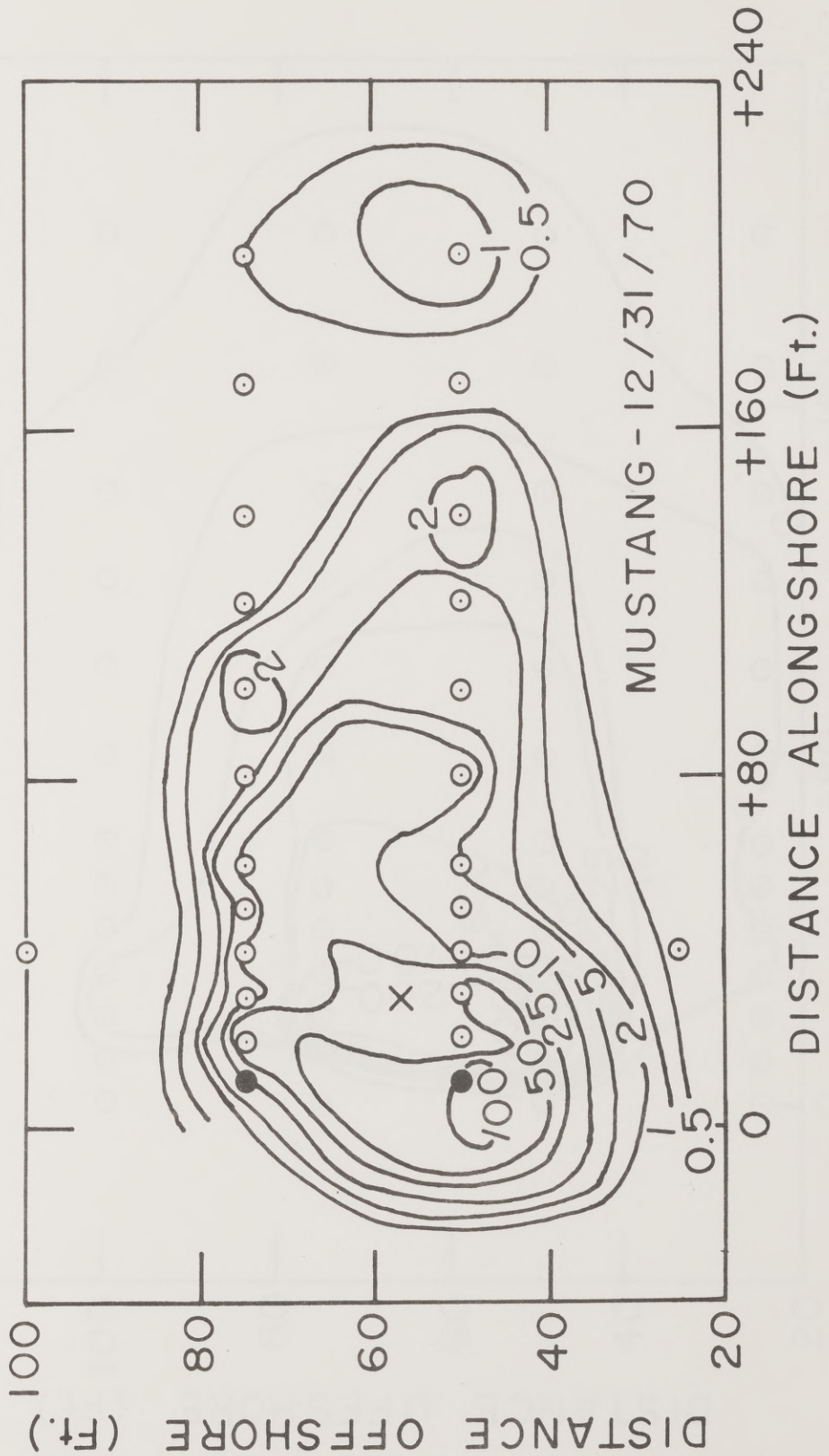
MUSTANG - 12/31/70
DISTANCE ALONGSHORE (Ft.)
DISTANCE OFFSHORE (Ft.)
+240
+160
+80
0
100
80
60
40
20
0.5
1
2
5
10
25
50
100

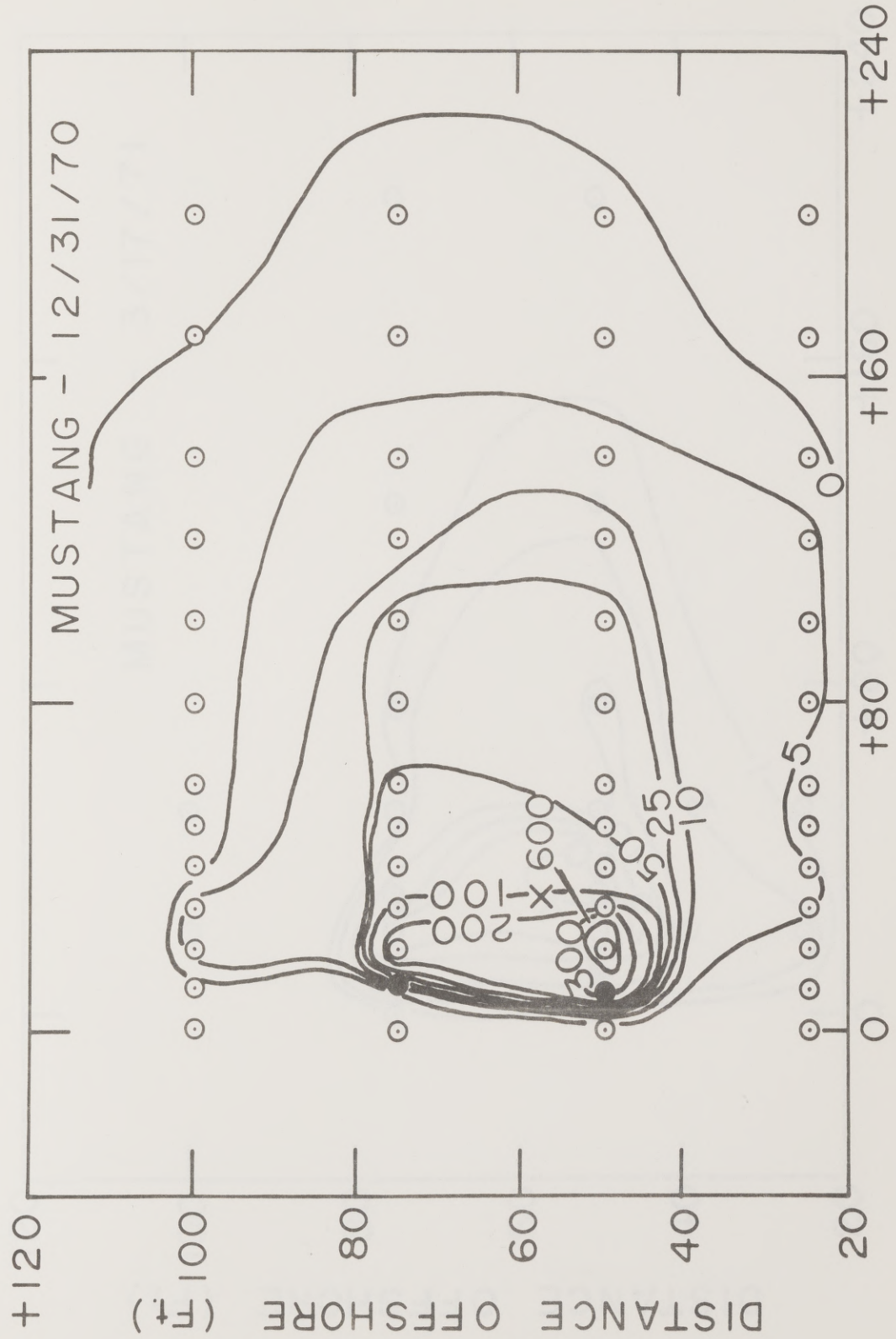
MUSTANG - 12/31/70
DISTANCE ALONGSHORE (Ft.)
DISTANCE OFFSHORE (Ft.)
+120
100
80
60
40
20
0
+80
+160
+240
0
5
10
25
50
100
200
300
600

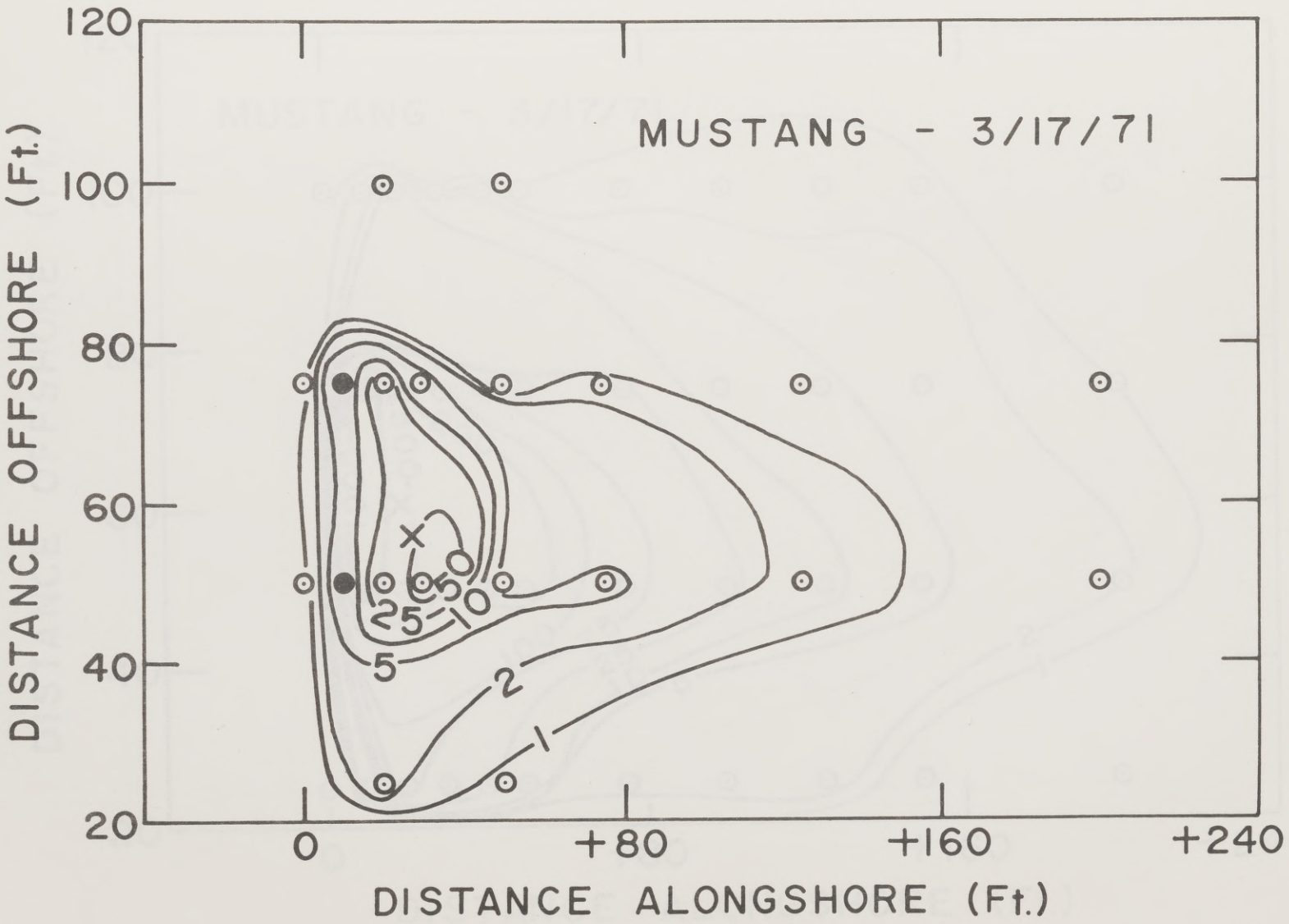
MUSTANG - 3/17/71
DISTANCE OFFSHORE (Ft.)
120
100
80
60
40
20
0
+80
+160
+240
DISTANCE ALONGSHORE (Ft.)
50
25
10
5
2
1

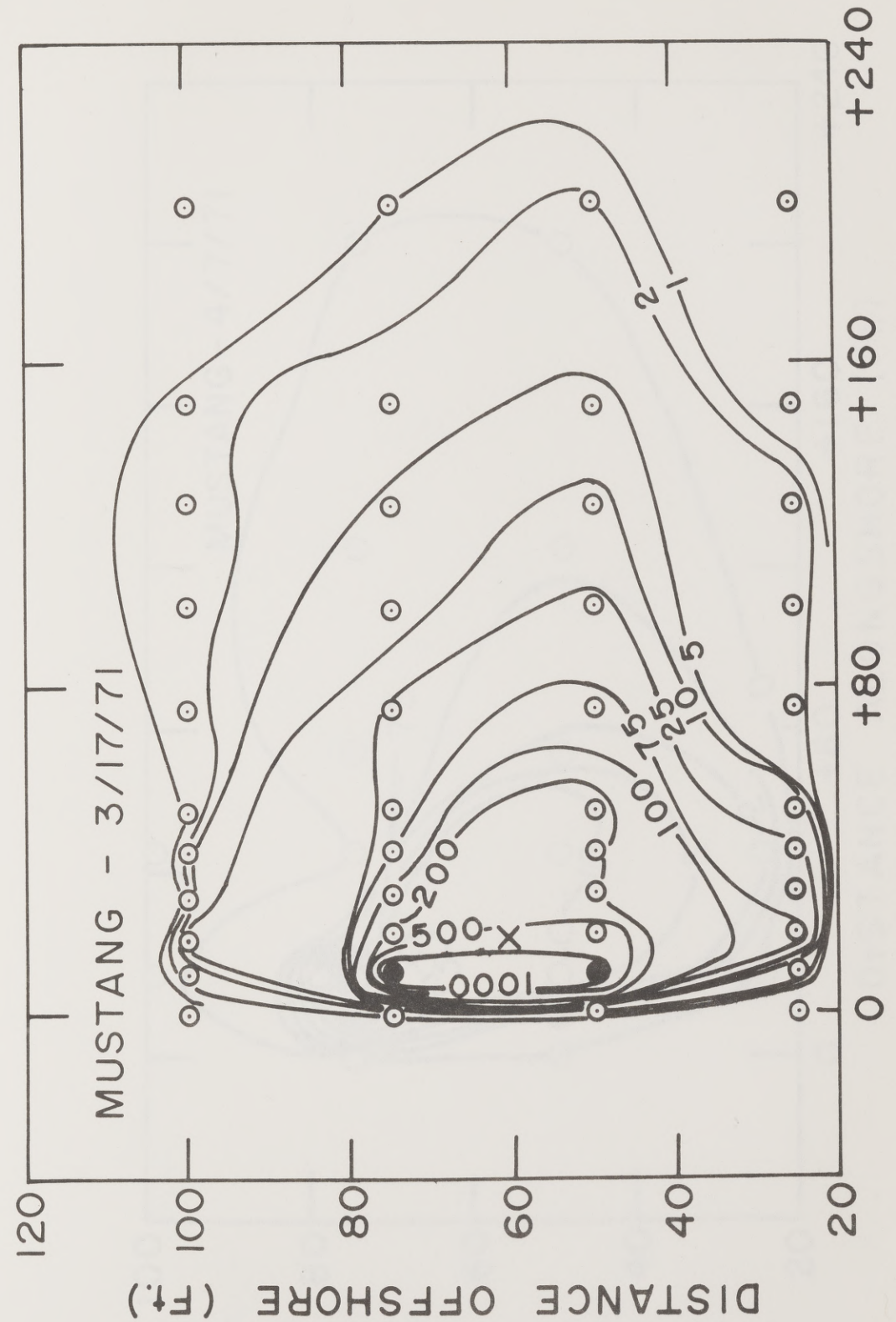
MUSTANG - 3/17/71
DISTANCE OFFSHORE (Ft.)
DISTANCE ALONGSHORE (Ft.)
120
100
80
60
40
20
0
+80
+160
+240
1
2
5
10
25
50
100
200
500
1000

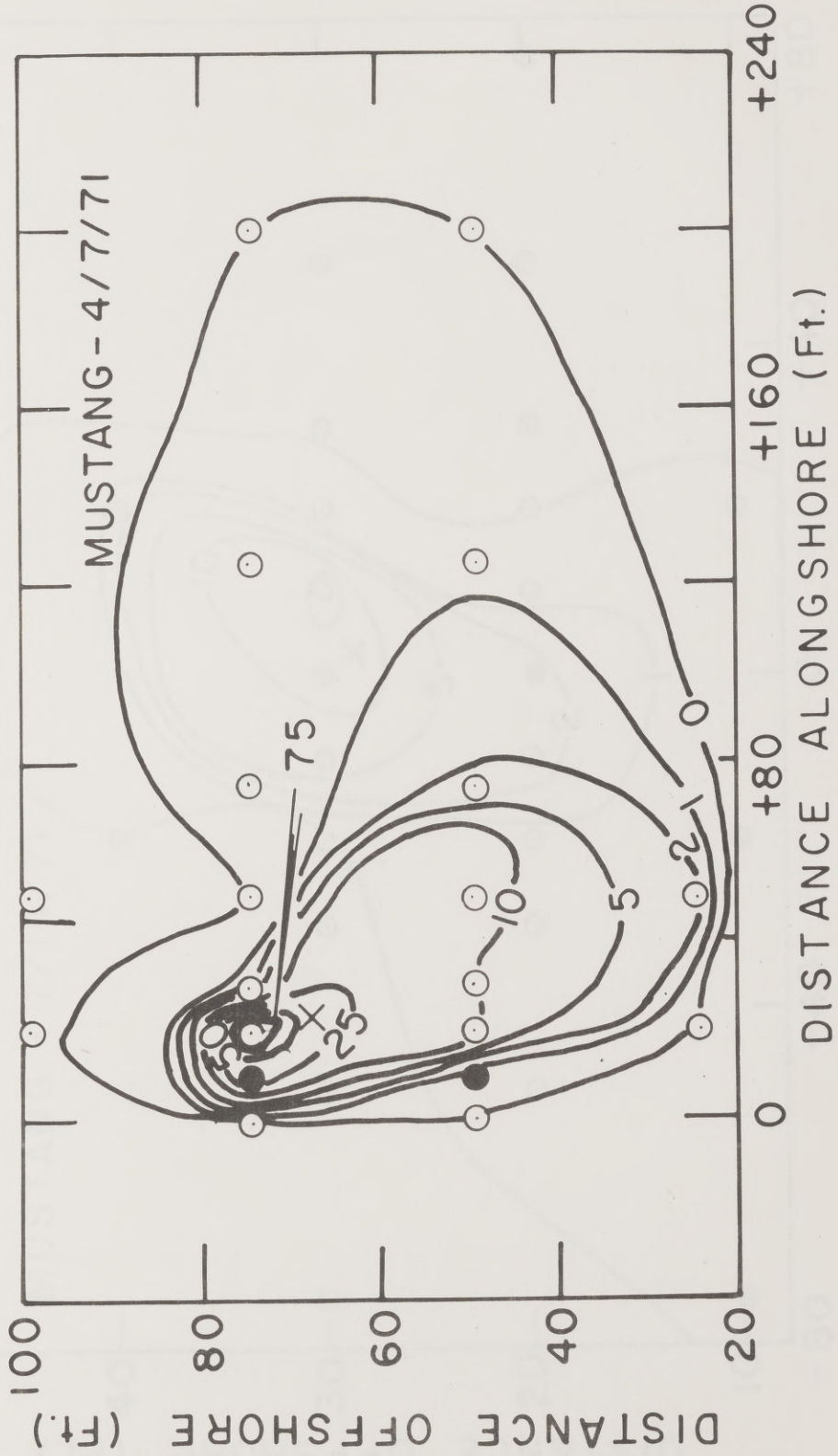
MUSTANG - 4/7/71
DISTANCE OFFSHORE (Ft.)
DISTANCE ALONGSHORE (Ft.)
100
80
60
40
20
0
+80
+160
+240
75
25
10
5
2
1
0

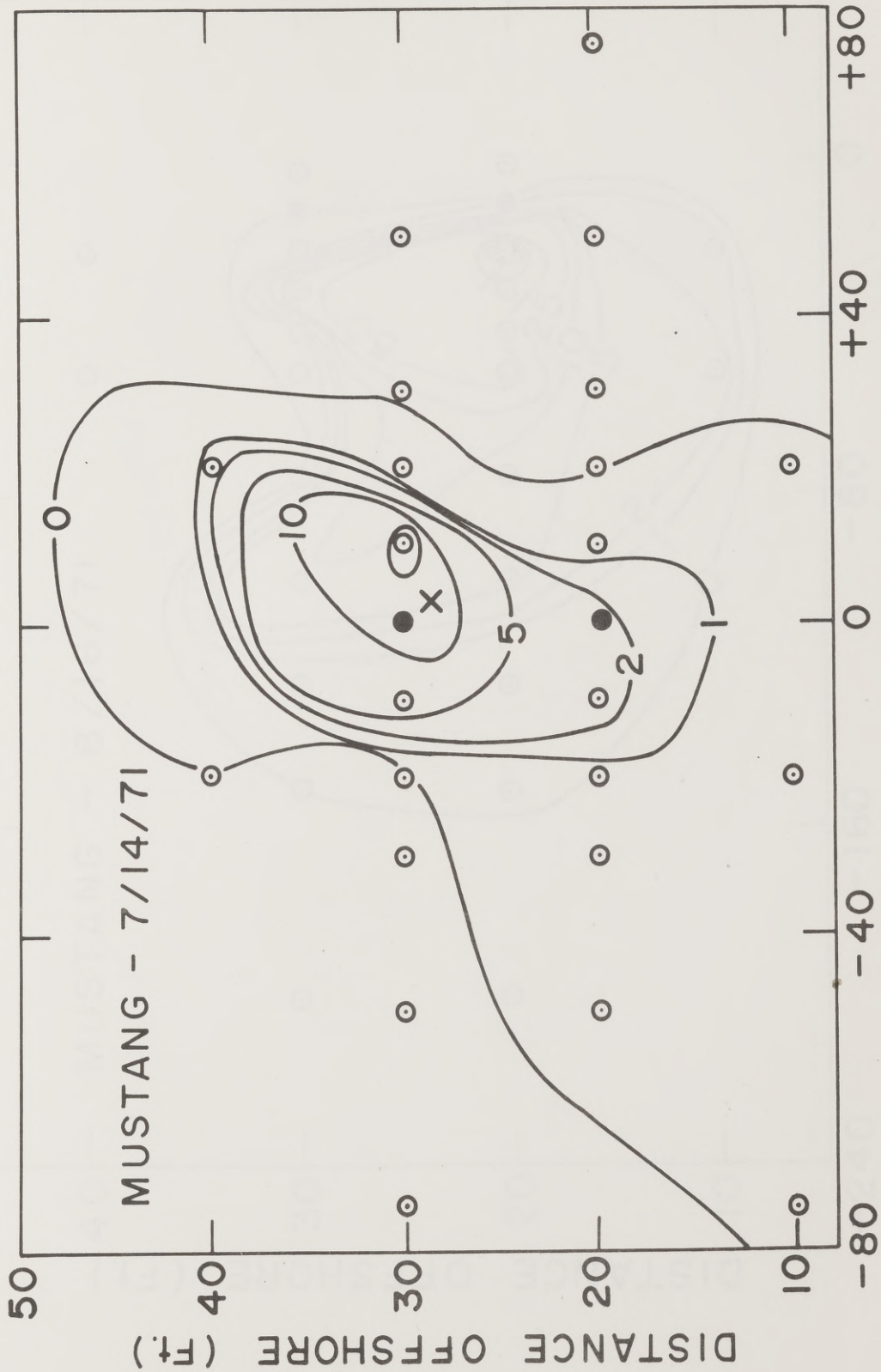
MUSTANG - 7/14/71
0
10
5
2
1
X
50
40
30
20
10
-80
-40
0
+40
+80
DISTANCE OFFSHORE (Ft.)
DISTANCE ALONGSHORE (Ft.)

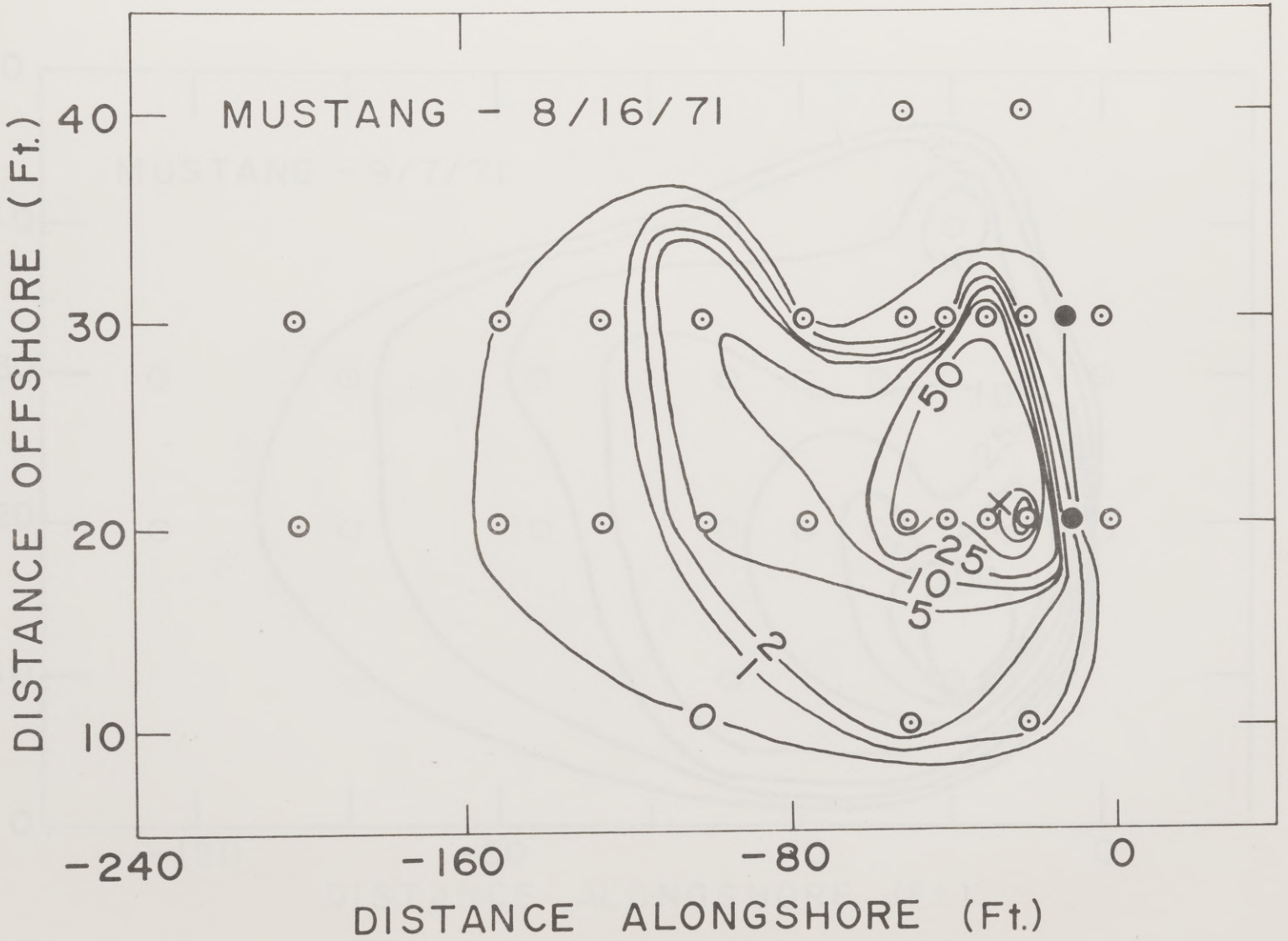
MUSTANG - 8/16/71
DISTANCE OFFSHORE (Ft.)
40
30
20
10
-240
-160
-80
0
DISTANCE ALONGSHORE (Ft.)
50
25
10
5
2
1
0

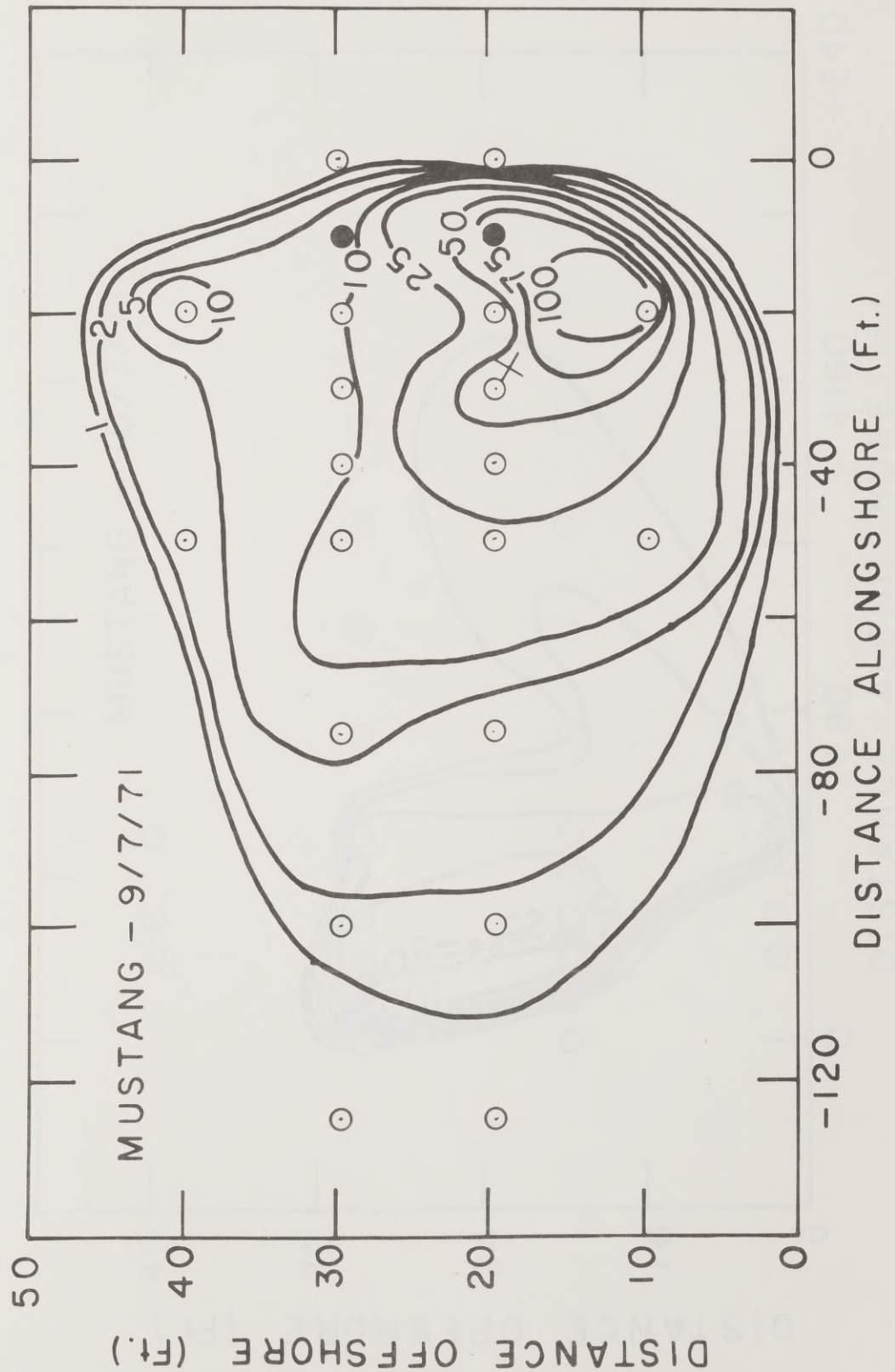
MUSTANG - 9/7/71
1
2
5
10
10
25
50
75
100
0
-40
-80
-120
DISTANCE ALONGSHORE (Ft.)
0
10
20
30
40
50
DISTANCE OFFSHORE (Ft.)

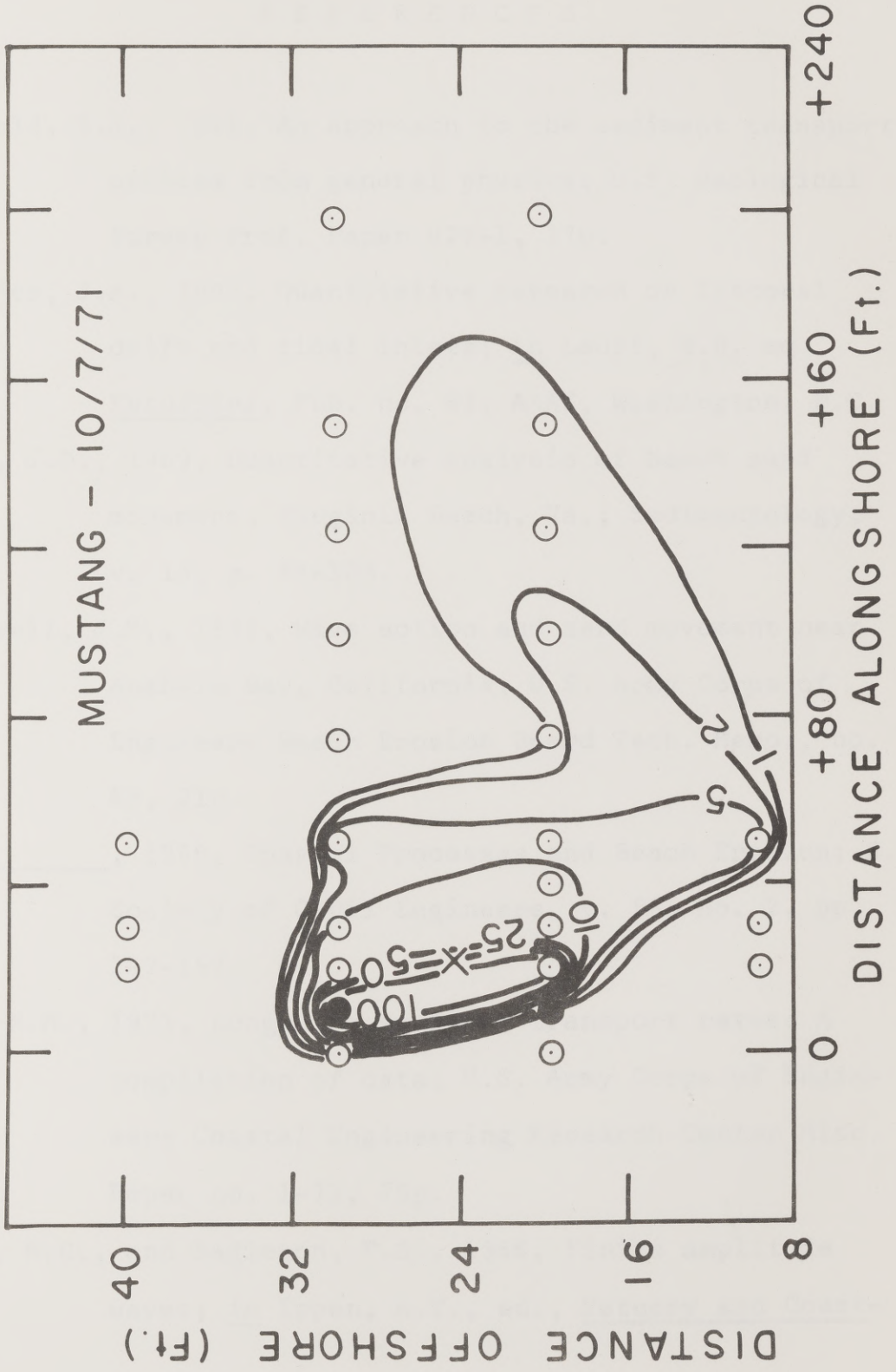
MUSTANG - 10/7/71
DISTANCE OFFSHORE (Ft.)
DISTANCE ALONGSHORE (Ft.)
0
+80
+160
+240
8
16
24
32
40
1
2
5
10
25=<X=<50
100

R E F E R E N C E S

Bagnold, R.A., 1966, An approach to the sediment transport problem from general physics; U.S. Geological Survey Prof. Paper 422-1, 37p.

Battjes, J.A., 1967, Quantitative research on littoral drift and tidal inlets; in Lauff, G.H. ed., Estuaries, Pub. no. 83, AAAS, Washington, D.C.

Boon, J.D., 1969, Quantitative analysis of beach sand movement, Virginia Beach, Va.; Sedimentology, v. 13, p. 85-103.

Caldwell, J.M., 1956, Wave action and sand movement near Anaheim Bay, California; U.S. Army Corps of Engineers Beach Erosion Board Tech. Memo., no. 68, 21p.

_____, 1966, Coastal Processes and Beach Erosion; J. Society of Civil Engineers, v. 53, no. 2, pp. 142-157.

Das, M.M., 1971, Longshore sediment transport rates: A compilation of data; U.S. Army Corps of Engineers Coastal Engineering Research Center Misc. Paper no. 1-71, 75p.

Dean, R.G., and Eagleson, P.S., 1966, Finite amplitude waves; in Ippen, A.T., ed., Estuary and Coast-

line Hydrodynamics, McGraw Hill, N.Y., 744p.

Duane, D.B., and Judge, C.W., 1969, Radioisotopic sand tracer study Point Conception, California; U.S. Army Corps of Engineers Coastal Engineering Research Center, Misc. Paper no. 2-69, 81p.

Duane, D.B., 1970, Tracing sand movement in the littoral zone: progress in the radioisotopic sand tracer (RIST) study - July 1968 - February 1969; U.S. Army Corps of Engineers Coastal Engineering Research Center, Misc. Paper no. 4-70, 52p.

Fairchild, J., 1966, Correlation of littoral transport with wave energy along shores of N.Y. and N.J.; U.S. Army Corps of Engineers Coastal Engineering Research Center Tech. Memo. no. 18, Wash. D.C.

Galvin, C.J., 1967, Longshore current velocity; a review of theory and data; Reviews of Geophysics, v.5, no. 3, pp. 287-304.

Gebhard, T.G., Jr., 1968, Numerical solutions of the two dimensional convective dispersion equation; unpub. PhD dissertation, University of Texas at Austin.

Holley, E.R., 1967, The concept and importance of diffusion; presented A.S.C.E. Environmental Engineering Conference, Dallas, Texas, Feb. 1967.

Ingle, J.C., 1966, The Movement of Beach Sand, Elsevier, Amsterdam, 221p.

Inman, D.L., and Bagnold, R.A., 1963, Littoral processes; in Hill, M.N. ed. The Sea; Ideas and Observations, v. 3, Interscience Publ., p. 529-553.

Inman, D.L., and Frautschy, J.D., 1966, Littoral processes and the development of shorelines; Coastal Engineering, p. 511-536, Amer. Soc. Civil Engr., N.Y.

Inman, D.L., Komar, P.D., and Bowen, A.J., 1968, Longshore transport of sand; Proc. Eleventh Conf. Coastal Engr., Council Wave Research.

Ippen, A.T. ed., 1966, Estuary and Coastline Hydrodynamics, McGraw Hill, N.Y., 744p.

Johnson, J.W., and Eagleson, P.S., 1966, Coastal Processes, in Ippen, A.T., ed., Estuary and Coastline Hydrodynamics, McGraw Hill, N.Y., 744p.

King, C.A.M., 1959, Beaches and Coasts, Arnold, London, 403p.

Komar, P.D., 1969, The longshore transport of sand on beaches, Ph.D. dissertation, The University of California at San Diego, 143p.

_____, 1971, The mechanics of sand transport on beaches; Jour. Geophys. Research, v. 76, no. 3, pp. 713-721.

_____, and Inman, D.L., 1969, The longshore transport of sand on beaches; Trans. Amer. Geophys. Union, v. 50, p. 191 (abs).

Komar, P.D., and Inman, D.L., 1970, Longshore sand transport on beaches; Jour. Geophys. Research, v. 75, no. 30, pp. 5914-5927.

Krumbein, W.C., 1944, Shore currents and sand movement on a model beach; U.S. Army Corps of Engineers Beach Erosion Board Tech. Memo. no. 7, 43p.

Moore, G.W., and Cole, J.Y., 1960, Coastal processes in the vicinity of Cape Thompson, Alaska, in Kachedoorian, R., et al., Geological Investigations in Support of Project Chariot in the Vicinity of Cape Thompson, U.S. Geological Survey Trace Elements Investigations Report 753, pp. 41-54.

Putnam, J.A., Munk, W.H., and Traylor, M.A., 1949, The prediction of longshore currents; Trans. Amer. Geophys. Union, v. 30, p. 337-345.

Sauvage de Saint Marc, G. and Vincent, G., 1954, Transport littoral de fleches et de tombolos; Proc. Fifth Conf. Coastal Engineering, Council Wave Research pp. 296-328.

Savage, R.P., 1962, Laboratory determination of littoral transport rates; Jour. Waterways and Harbors Div. Amer. Soc. Civ. Engr., v. 88, pp. 69-72.

Saville, T. Jr., 1950, Model study of sand transport along an infinitely long straight beach; Amer. Geophys. Union Trans., v. 31, pp. 555-565.

Shay, E.A., and Johnson, J.W., 1951, Model studies on the movement of sand transported by wave action along a straight beach, Issue 7, series 14, Inst. of Engineering Research, Univ. California at Berkely, (unpub).

Sheppard, C.W., 1962, Basic Principles of the Tracer Method, Wiley and Sons, N.Y., 282p.

Sverdrup, H.U., and Munk, W.H., 1947, Wind Sea and Swell: Theory of Relations for Forecasting, H.O. Pub. no. 601, U.S. Hydrographic Office, 44p.

Teleki, P.G., 1962, A summary of the production and scanning of fluorescent tracers: Federal Interagency Sedimentation Conf. Proc., Jackson, Miss. 11p.

U.S. Army Corps of Engineers Coastal Engineering Research Center, 1966, Shore Protection Planning and Design, Tech. Rept. no. 4, 3rd. edition.

Watts, G.M., 1953, A study of sand movement at South Lake Worth Inlet, Florida; U.S. Army Corps of Engineers Beach Erosion Board, Tech. Memo. no. 42.

Williams, L,C., 1969, CERC wave gages; U.S. Army Corps of Engineers Coastal Engineering Research Center Tech. Memo. no. 30, 117p.

Wright, F.F., 1962, The development and application of a fluorescent marking technique for tracing sand movement on beaches; Tech. Rept. no. w, Proj. N.R. 388-057, Contract NONR 266(68), Office of Naval Research, Geography Branch, Wash. D.C.

Yasso, W.E., 1964, Use of fluorescent tracers to determine foreshore sediment transport, Sandy Hook, N.J., Tech. Rept. no. 6, of Proj. N.R. 388-057, Office of Naval Research, Geography Branch.

The vita has been removed from the digitized version of this document.